Article

IL-3 orchestrates ulcerative colitis pathogenesis by controlling the development and the recruitment of splenic reservoir neutrophils

Graphical abstract
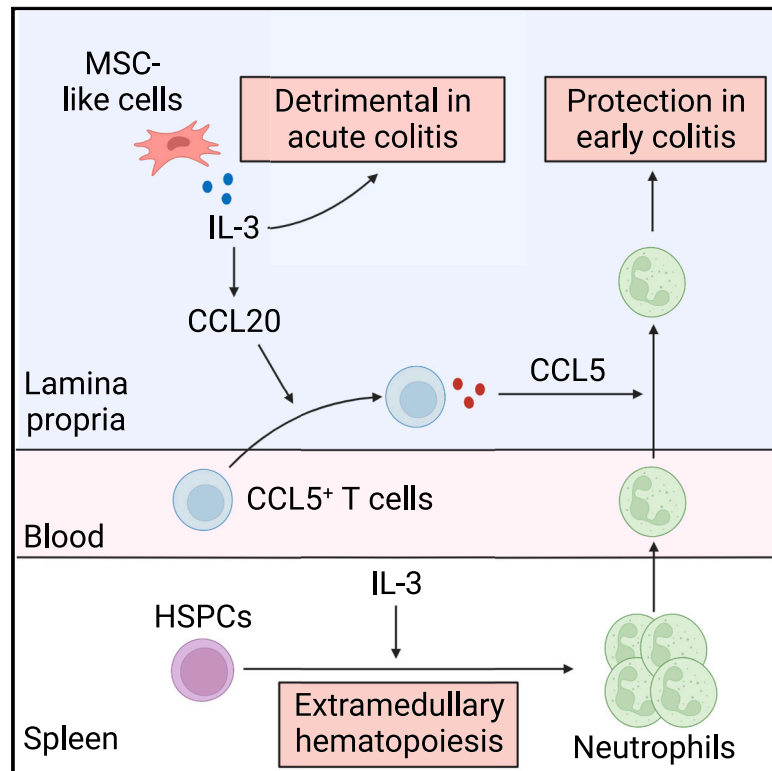
Authors

Alan Bénard, Anke Mittelstädt, Bettina Klösch, ..., Kai Sohn, Robert Grützmann, Georg F. Weber

Correspondence

alan.benard@uk-erlangen.de (A.B.), georg.weber@uk-erlangen.de (G.F.W.)

In brief

Bénard et al. show that interleukin-3 (IL-3) has a beneficial role at the onset of colitis by promoting the early recruitment of splenic neutrophils in a CCL5+ PD-1high LAG-3high T cell-, STAT5-, and CCL20-dependent manner, whereas IL-3 has a detrimental effect during severe colitis by amplifying inflammation.

Highlights

- IL-3 protects at the onset of colitis but is detrimental during acute colitis

- Spleen acts as an IL-3-dependent emergency reservoir for neutrophils during colitis

- IL-3 protection requires CCL5+ PD-1hi LAG-3hi T cells, STAT5 signaling, and CCL20

- IL-3 is produced by MSC-like cells in the colon

CellPress

Article

IL-3 orchestrates ulcerative colitis pathogenesis by controlling the development and the recruitment of splenic reservoir neutrophils

Alan Bénard,[1,5,*] Anke Mittelstädt,[1] Bettina Klösch,[1] Karolina Glanz,[2] Jan Müller,[2] Janina Schoen,[3] Björn Nüse,[4] Maximilian Brunner,[1] Elisabeth Naschberger,[1] Michael Stürzl,[1] Jochen Mattner,[4] Luis E. Muñoz,[3] Kai Sohn,[2] Robert Grützmann,[1] and Georg F. Weber[1,*]

[1]Department of Surgery, Universitätsklinikum Erlangen, Friedrich-Alexander Universität Erlangen-Nürnberg, Erlangen, Germany
[2]Fraunhofer Institute for Interfacial Engineering and Biotechnology, Stuttgart, Germany
[3]Department of Internal Medicine 3 - Rheumatology and Immunology, Friedrich-Alexander-Universität Erlangen-Nürnberg and Universitätsklinikum Erlangen, Erlangen, Germany
[4]Mikrobiologisches Institut-Klinische Mikrobiologie, Immunologie und Hygiene, Universitätsklinikum Erlangen and Friedrich-Alexander-Universität (FAU), Erlangen, Germany
[5]Lead contact
*Correspondence: alan.benard@uk-erlangen.de (A.B.), georg.weber@uk-erlangen.de (G.F.W.)
https://doi.org/10.1016/j.celrep.2023.112637

SUMMARY

Inflammatory bowel diseases (IBDs) are a global health issue with an increasing incidence. Although the pathogenesis of IBDs has been investigated intensively, the etiology of IBDs remains enigmatic. Here, we report that interleukin-3 (*Il-3*)-deficient mice are more susceptible and exhibit increased intestinal inflammation during the early stage of experimental colitis. IL-3 is locally expressed in the colon by cells harboring a mesenchymal stem cell phenotype and protects by promoting the early recruitment of splenic neutrophils with high microbicidal capability into the colon. Mechanistically, IL-3-dependent neutrophil recruitment involves CCL5^{+} PD-1^{high} LAG-3^{high} T cells, STAT5, and CCL20 and is sustained by extramedullary splenic hematopoiesis. During acute colitis, *Il-3*^{−/−} show, however, increased resistance to the disease as well as reduced intestinal inflammation. Altogether, this study deepens our understanding of IBD pathogenesis, identifies IL-3 as an orchestrator of intestinal inflammation, and reveals the spleen as an emergency reservoir for neutrophils during colonic inflammation.

INTRODUCTION

Inflammatory bowel diseases (IBDs) such as ulcerative colitis (UC) and Crohn's disease are inflammatory disorders of the intestinal tract with increasing worldwide morbidity.[1] The pathogenesis of IBDs is not fully understood. It involves a causative combination of environmental, genetic, and microbial factors resulting in an aberrant mucosal immune response driven by microbial factors of the commensal flora.[2,3] Therapies against IBDs rely on immunosuppressive molecules, leukocyte trafficking inhibitors, or application of mesenchymal stem cells.[4] However, current treatments are not effective in all patients, as a significant number of patients relapse.[5] Thus, a better comprehension of the mechanisms involved in IBD pathogenesis might lead to the development of novel therapies.

Interleukin-3 (IL-3), mainly produced by immune cells,[6–10] is a hematopoietic growth factor playing a key role during inflammatory diseases by promoting either the survival, the differentiation, the proliferation, or the recruitment of leukocytes.[11–13] Depending on the type of disease and course of inflammation, IL-3 can be either detrimental or beneficial. For instance, IL-3 fuels the

cytokine storm in sepsis, resulting in increased mortality,[9] whereas IL-3 limits Alzheimer's disease by reprogramming microglia.[10] Although the expression of IL-3 and CD123, the IL-3 receptor α-chain, were previously reported in colon,[1,14] the role of IL-3 during IBDs remains unknown.

Neutrophils play a crucial role at the initiation of IBDs. They are rapidly recruited into the injured intestinal epithelium and protect against translocated pathogens by releasing inflammatory mediators into the microenvironment, by pathogen phagocytosis, or by inducing neutrophil extracellular traps.[15] However, the persistent accumulation of neutrophils might potentiate and perpetuate intestinal tissue damage and barrier integrity destruction,[16] converting neutrophils into key orchestrators of intestinal inflammation and IBD-related complications.

The aim of our study was to investigate the role of IL-3 during IBDs. Here, we report that the contribution of IL-3 in IBDs depends on the level of intestinal inflammation. *Il-3*-deficient mice were more susceptible to dextran sulfate sodium (DSS)-induced colitis compared with control mice during the early stages of colitis, with the protective role of IL-3 involving the early recruitment of splenic neutrophils with high microbicidal capability in a CCL5^{+} PD-1^{+}
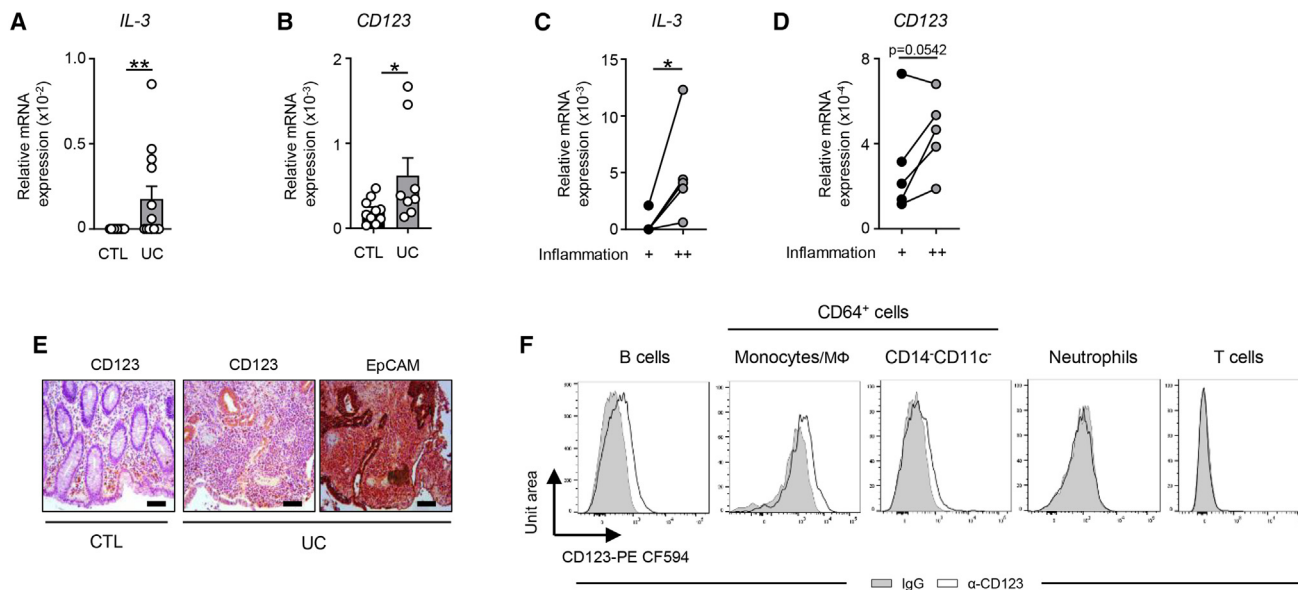
Figure 1. IL-3 and CD123 are expressed in the colon of patients with UC

(A) Relative mRNA expression of *IL-3* in control colon (n = 11) and in the colon of patients with UC (n = 13).

(B) Relative mRNA expression of *CD123* in control colon and in the colon of patients with UC (n = 8–10).

(C) Relative mRNA expression of IL-3 in colon from the same UC patient with either low (+) or high (++) levels of inflammation (n = 5). The inflammation levels low (+) and high (++) were assessed through the expression of *TNF* and the percentage of neutrophils in the colon.

(D) Relative mRNA expression of CD123 in colon from the same patient with UC with either low (+) or high (++) levels of inflammation (n = 6).

(E) Immunochemistry of CD123 and EpCAM in the colon of patients with UC or in control colon. Scale bar, 50 μm (n = 4–7).

(F) Representative histogram of CD123 expression at the surface of B cells, CD64$^+$ monocytes/macrophages, CD64$^+$CD14$^-$CD11c$^-$ cells, neutrophils, and T cells in the colon of patients with UC (n = 11).

Data are pooled data from at least 2 independent experiments. Data represent mean ± SEM and were analyzed by the two-tailed unpaired (A and B) or paired (C and D) t test. *p < 0.05; **p < 0.01.

LAG-3$^+$ T cell-, STAT5-, and CCL20-dependent manner. However, IL-3 was detrimental during acute colitis by amplifying intestinal inflammation.

RESULTS

Colon tissues of patients with UC harbor IL-3 and CD123

To address a potential contribution of IL-3 in the pathogenesis of IBDs, we first assessed the expression of IL-3 and CD123, the IL-3 receptor α-chain, in colon tissues of patients with UC and control patients without IBDs. Patients with UC exhibited increased *IL-3* and *CD123* mRNA expression in the inflamed colon as compared to controls (Figures 1A and 1B; Table S1). Further analysis showed that *IL-3* and *CD123* mRNA expression levels in the colon of patients with UC correlated with the degree of colonic inflammation (Figures 1C and 1D). Furthermore, CD123 was expressed in the colon by epithelial cells (Figure 1E) and infiltrating immune cells such as CD19$^+$ B cells, CD64$^+$ CD11c$^+$ CD14$^+$ monocytes/macrophages, and CD64$^-$ CD15$^-$ CD11c$^{-/low}$ CD123$^+$ plasmacytoid dendritic cells (pDCs) (Figures 1F and S1), suggesting, therefore, that IL-3 might have a pleiotropic effect during UC.

IL-3 protects during the early phase of DSS-induced colitis

To investigate the function of IL-3 during IBDs, we induced colitis in wild-type (WT) and *Il-3*-deficient mice (*Il-3$^{-/-}$*) using DSS, a

well-studied chemical murine model of colitis mimicking human IBDs in multiple aspects, including cytokine dysregulation.[17] *Il-3$^{-/-}$* mice exhibited reduced survival (Figure 2A), and the surviving mice suffered from pronounced weight loss (Figure 2B). Interestingly, *Il-3$^{-/-}$* mice displayed higher disease severity only during the early stage of colitis compared with WT controls (Figure 2C). In addition, *Il-3$^{-/-}$* mice displayed increased plasma tumor necrosis factor α (TNF-α) levels (Figure 2D) only 1 day after the onset of colitis compared with WT mice. *Il-3$^{-/-}$* mice also showed increased *Tnfα* mRNA expression (Figure 2E) in colon tissues during the early stage of colitis and increased colonic mucosa thickness (Figure 2F) 4 days after DSS application. At steady state, as well as 1 and 4 days after colitis induction, *Il-3$^{-/-}$* mice harbored a reduced number of Ly6G^{high} Ly6C$^+$ CD11b$^+$ F4/80$^-$ neutrophils in the colon (Figure 2G). No differences were, however, observed after 7 days. Altogether, our results indicated that IL-3 protects during the early phase of the disease and suggested that IL-3 modulates innate immune mechanisms involved in the development of intestinal inflammation. To confirm this hypothesis, we infected WT and *Il-3$^{-/-}$* mice with *S. typhimurium*, a bacteria that causes colitis. *Il-3$^{-/-}$* mice exhibited increased bacterial colony-forming units (CFUs) in liver and feces 4 days after *S. typhimurium* infection (Figure S2A) compared with controls as well as increased numbers of leukocytes (Figure S2B) and increased *Il-17a* mRNA expression in the colon (Figure S2C). Thus, these results confirm the role of IL-3 on
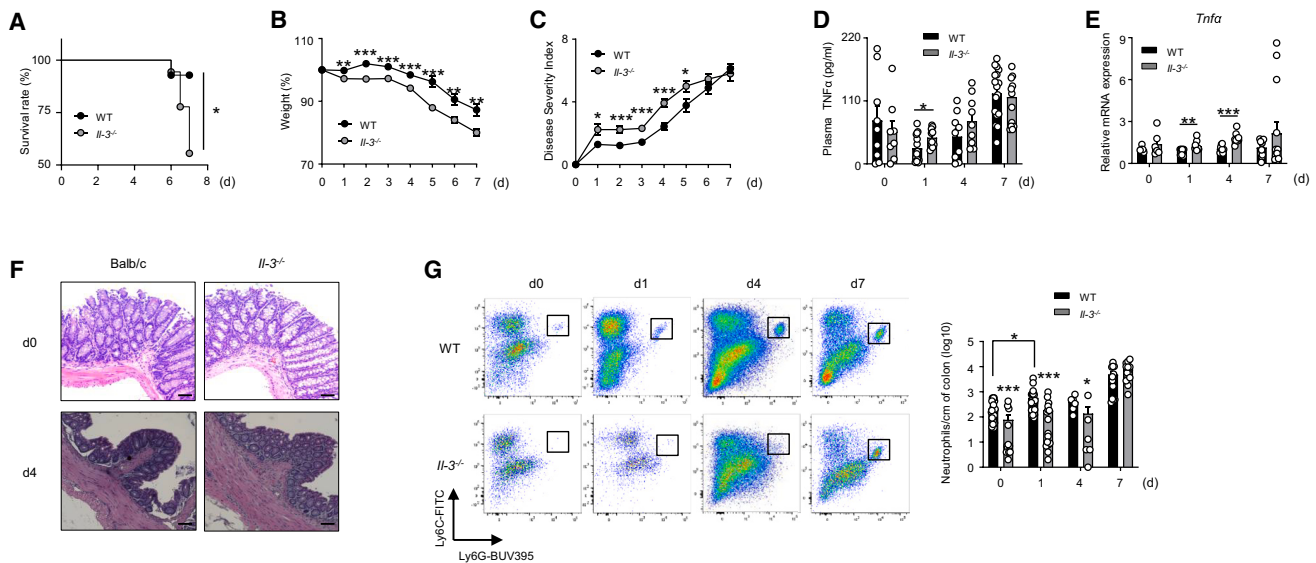
Figure 2. IL-3 limits the development of experimental colitis

(A) Survival curve of WT and $Il\text{-}3^{-/-}$ mice upon DSS application (n = 14–18 per group). Data were analyzed by log rank (Mantel-Cox) test.

(B) Comparison of weight loss of WT and $Il\text{-}3^{-/-}$ mice upon DSS treatment (n = 18–19 per group).

(C) Severity index of WT and $Il\text{-}3^{-/-}$ mice following DSS colitis induction (n = 13–14 per group).

(D) Levels of plasma TNF in WT and $Il\text{-}3^{-/-}$ mice 0, 1, 4, and 7 days after DSS administration (n = 8–17 per group).

(E) Relative mRNA expression of $Tnf\alpha$ in colon of WT and $Il\text{-}3^{-/-}$ mice 0, 1, 4 and 7 days after DSS administration; the expression level was arbitrarily set to 1 for one sample from the WT group (for each time), and the values for the other samples were calculated relatively to this reference (n = 3–14 per group).

(F) Representative hematoxylin and eosin staining of colon tissues from WT and $Il\text{-}3^{-/-}$ mice at steady state and 4 days after DSS administration. Scale bar, 100 μm (n = 3–5 per group).

(G) Representative fluorescence-activated cell sorting (FACS) dot plots and enumeration of neutrophils in colon of WT and $Il\text{-}3^{-/-}$ mice 0, 1, 4, and 7 days after DSS administration (n = 6–31 per group).

Data represent mean ± SEM and were analyzed by the two-tailed unpaired t test (B–E and G). *p < 0.05; **p < 0.01; ***p < 0.001.

intestinal innate immunity and indicate a pivotal role of IL-3 in the inhibition of bacterial replication and translocation.

Early protection requires splenic reservoir neutrophils

During the initial phase of intestinal inflammation, neutrophils are the first immune cells migrating into the inflammatory site.[16] In addition to the reduced number of neutrophils observed in the colon of $Il\text{-}3^{-/-}$ mice compared with WT mice (Figure 2G), we found that the number of neutrophils increased in the colon of WT mice 1 day after DSS-induced colitis, whereas no increase was observed in $Il\text{-}3^{-/-}$ mice (Figure 2G). Furthermore, the $Il\text{-}3$ mRNA expression in the colon was also positively correlated with the number of colonic neutrophils in WT mice (Figure S3A). We therefore investigated whether the IL-3-mediated protection at the onset of colitis was associated with an improved neutrophil recruitment into the colon. The depletion of neutrophils by the administration of anti-Ly6G antibodies in WT mice resulted in increased weight loss upon DSS application compared with control immunoglobulins (Figures 3A and S3B), whereas no difference was observed between both $Il\text{-}3^{-/-}$ mouse cohorts (Figure S3C), suggesting that IL-3 limits the development of colitis due to the early recruitment of neutrophils into the colon. This recruitment was mediated through the IL-3 receptor common β-chain (CD131), as reduced neutrophil numbers were recovered from the colon of $Cd131^{-/-}$ mice following DSS application (Figure 3B). Remarkably, sple-

nectomized (Sx) WT mice displayed a pronounced weight loss (Figure 3C), higher plasma TNF-α levels (Figure 3D), and increased neutrophil numbers (Figure 3E) in the colon 1 day after DSS-induced colitis compared with sham WT mice, indicating that the spleen protects against colonic inflammation at the onset of colitis. By contrast, no differences were observed between sham and Sx $Il\text{-}3^{-/-}$ mice (Figures 3C–3E). Likewise, no difference in weight loss was observed in sham or Sx WT mice that received a combination of neutralizing antibodies against CXCL1 and CXCL2 intravenously (Figure 3F), the two main chemokines involved in neutrophil mobilization from the bone marrow (BM).[18] In addition, we observed that the number of neutrophils increased in the colon of sham WT mice, but not in Sx WT mice, 6 h after the onset of DSS-induced colitis, indicating an early recruitment of splenic neutrophils into the colon following DSS challenge (Figure 3G). Interestingly, the adoptive transfer of splenic neutrophils from WT donors into Sx WT recipient mice resulted in reduced plasma TNF-α levels (Figure 3H) and decreased neutrophil numbers in colon (Figure 3I) at day 1 after DSS application. whereas the adoptive transfer of neutrophils from BM led only to decreased neutrophil numbers in colon (Figure 3I). Collectively, these results indicate that IL-3 protects at the onset of colitis through the early recruitment of splenic neutrophils and suggest that splenic neutrophils and neutrophils from BM are functionally different. To better characterize differences between neutrophils from spleen and
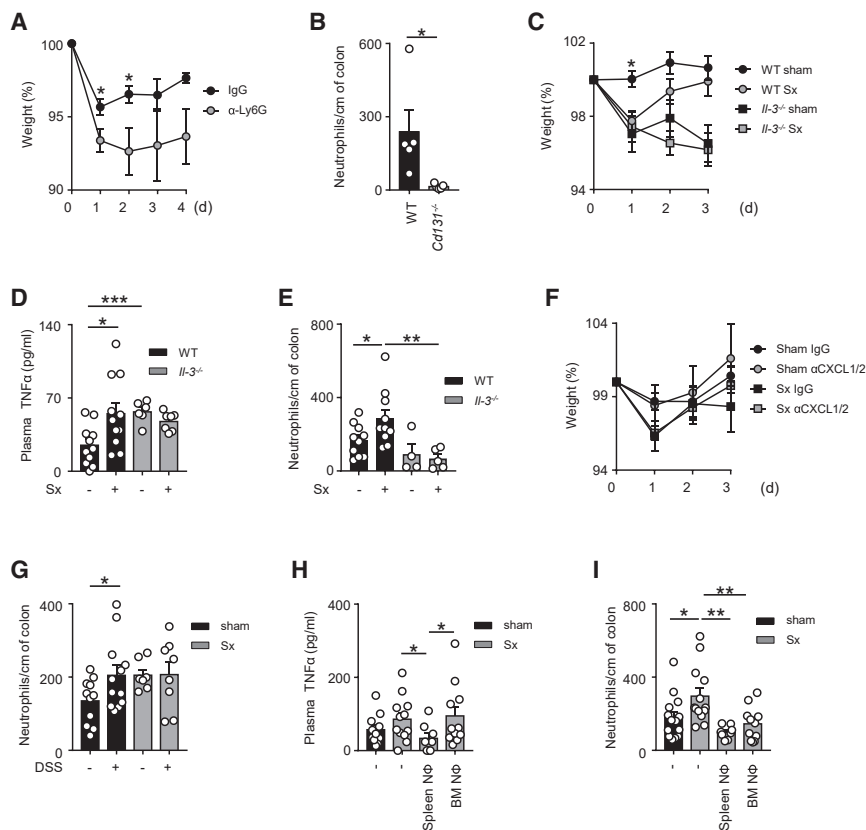
Figure 3. IL-3 promotes early splenic neutrophil recruitment into the colon during experimental colitis

(A) Comparison of weight loss in DSS-treated WT mice that either received an intravenous injection of anti-Ly6G or isotype control antibody (n = 7–8 per group).

(B) Enumeration of neutrophils in colon of WT and $Cd131^{-/-}$ mice 1 day after DSS administration (n = 5 per group).

(C) Comparison of weight loss of sham or splenectomized WT and $Il-3^{-/-}$ mice upon DSS (n = 5–17 per group).

(D) Levels of plasma TNF-α in sham or splenectomized WT and $Il-3^{-/-}$ mice 24 h after DSS administration (n = 6–11 per group).

(E) Enumeration of neutrophils in colon tissues from sham or splenectomized WT and $Il-3^{-/-}$ mice 24 h after DSS administration (n = 4–10 per group).

(F) Comparison of weight loss in DSS-treated sham or splenectomized WT mice that either received an intravenous injection of a cocktail of anti-CXCL1 and anti-CXCL2 antibodies or an intravenous injection of isotype controls (n = 4–6 per group).

(G) Enumeration of neutrophils in colon tissues from sham or splenectomized WT mice 6 h after DSS administration (n = 7–12 per group).

(H and I) Levels of plasma TNF-α (H) and enumeration of neutrophils in colon (I) of sham or splenectomized WT mice in which neutrophils from spleen or bone marrow (BM) of WT mice were adoptively transferred 3 h after the onset of DSS-induced colitis. Mice were sacrificed 21 h later (n = 8–14 per group).

Data are pooled data from at least 2 independent experiments. Data represent mean ± SEM and were analyzed by the two-tailed unpaired t test (A–G), the Kruskal-Wallis test, or the Tukey's multiple comparison test (H and I). *p < 0.05; **p < 0.01; ***p < 0.001.

BM of naive WT mice, we performed RNA sequencing (RNA-seq) analysis. In order to exclude neutrophil progenitors, we only sorted neutrophils with high Ly6G expression as described in Xie et al.[19] (Figure S3D). RNA-seq analysis revealed 4,907 differentially expressed genes, 2,932 being higher in spleen and 1,975 being higher in BM (Figures 4A and 4B), confirming a previous study showing that neutrophils exhibited organ-specific transcriptome features.[19] We confirmed these results at the protein level and detected increased expression of adhesion molecules such as CD11b, chemokine receptors including CCR1, CCR3, and CCR6, and immunomodulatory molecules (PD-L1, CD64) in splenic neutrophils from naive WT mice (Figure 4C). We also observed that splenic neutrophils produced higher levels of reactive oxygen species (ROS) than neutrophils from BM 30 min after *ex vivo* PMA stimulation (Figure 4D). Increased elastase activity was detected in the supernatant 3 h after *ex vivo* lipopolysaccharide (LPS) stimulation of splenic neutrophils compared with neutrophils from BM (Figure 4E), and higher numbers of splenic IL-1β+ and TNF-α+ neutrophils—but not IL-10+ neutrophils—were identified 4 h after *ex vivo* stimulation with LPS (Figure 4F). Thus, our data indicate that splenic neutrophils display higher antimicrobial activity than neutrophils from BM, suggesting that the spleen might act as an emergency reservoir for neutrophils during intestinal inflammation.

Early neutrophil influx into the colon requires CCL5-expressing CD3+ T cells and CCL20

We next characterized the mechanism utilized by IL-3 to promote the influx of splenic neutrophils into the colon. The analysis of the mRNA expression of chemokines contributing to neutrophil recruitment showed that *Ccl5* was increased in the colon of DSS-treated WT mice compared with naive WT controls and DSS-treated $Il-3^{-/-}$ mice 1 day after the induction of colitis (Figures 5A and S3E). As well, patients with UC exhibited increased *CCL5* mRNA expression in the inflamed colon compared with controls (Figure 5B). *Ccl5* mRNA expression in the colon correlated with the numbers of colonic neutrophils and with colonic *Il-3* mRNA expression (Figures 5C and S3F). In addition, the antibody-mediated depletion of CCL5 resulted in reduced colonic neutrophil numbers 1 day after the onset of colitis (Figure 5D) as well as pronounced weight loss (Figure 5E) and enhanced *Tnfa* mRNA expression in the colon (Figure 5F). Using a Transwell membrane assay, we observed that CCL5 has a low capacity to recruit splenic neutrophils compared with CXCL1 and CXCL2 (Figures S3G–S3I), which is consistent with the study of Hwaiz et al.[20] However, we observed that *Cxcl1* and *Cxcl2* are barely expressed in the colon of naive mice and after 1 day of DSS-induced colitis compared with *Ccl5* (Figure S3J), suggesting that CCL5 might attract directly splenic neutrophils despite a low chemotaxis capacity. It is
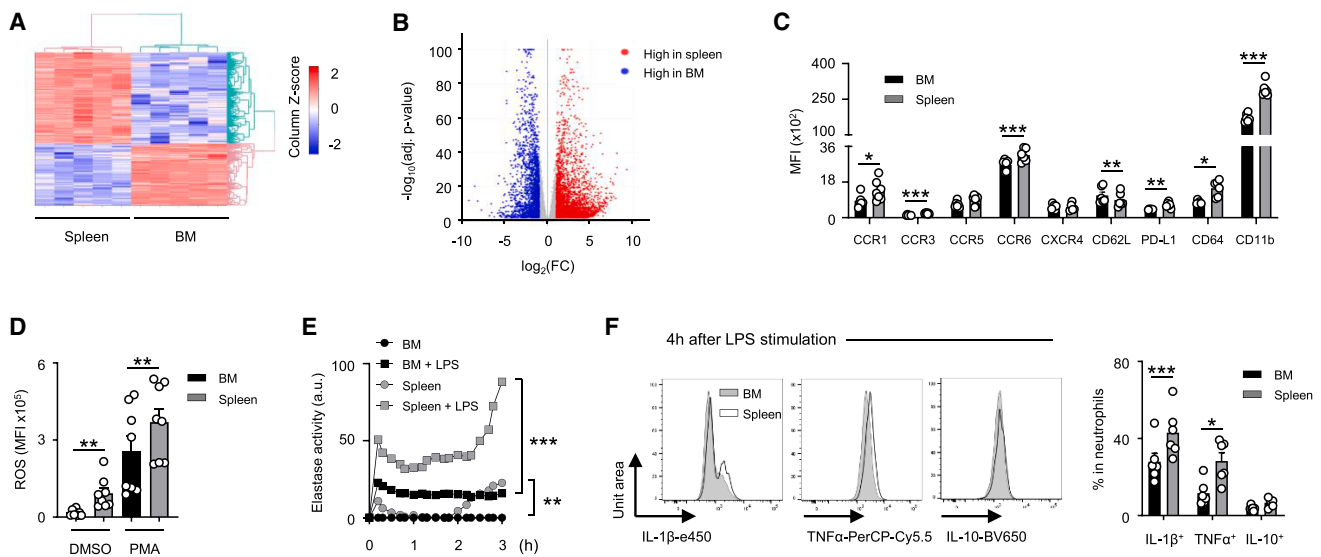
Figure 4. Splenic neutrophils are more pro-inflammatory than neutrophils from BM

(A) Heatmap of the differentially expressed genes between splenic and medullar neutrophils from naive mice (n = 5 per group).

(B) Volcano plot representation showing genes increased in splenic neutrophils compared with neutrophils from BM (n = 5 per group).

(C) Mean fluorescence intensity (MFI) of markers expressed at the surface of neutrophils from spleen and BM of WT naive mice (n = 6–7 per group).

(D) Reactive oxygen species neutrophils from spleen and BM of naive mice 30 min after stimulation with PMA or its vehicle (DMSO) (n = 8 per group).

(E) Elastase activity in supernatants of neutrophils from spleen and BM of naive mice stimulated *ex vivo* with LPS for 3 h compared with unstimulated controls (n = 6 per group).

(F) Representative histograms and percentages of neutrophils from spleen or BM of naive mice expressing IL-1β, TNF-α, or IL-10 4 h after *ex vivo* stimulation with LPS (n = 6 per group).

Data are pooled data from at least 2 independent experiments. Data represent mean ± SEM and were analyzed by the two-tailed paired (C, D, and F) t test or the Tukey's multiple comparison test (E). *p < 0.05; **p < 0.01; ***p < 0.001.

also possible that CCL5 promotes the recruitment of neutrophils into the colon in an indirect manner as previously described.[20] Flow cytometry analysis revealed that mainly $CD3^+$ T cells in the colon expressed CCL5 (Figures 5G and S4A). Likewise, the retrospective analysis of a single-cell RNA-seq atlas of colon biopsies from patients with UC[21] revealed that *CCL5* expression in colon tissue was also mainly associated with T cells (Figure 5H). $CCL5^+$ T cells were present in the colon of WT mice during steady state and increased 1 day after colitis induction by DSS (Figure 5I). Moreover, all the main subtypes of colonic T cells expressed CCL5, with $CD8^+$ T cells representing the main cellular CCL5 source (Figure S4B). Colonic $CCL5^+$ T cells exhibited higher expression of PD-1, LAG-3, and CCR7 compared with colonic $CCL5^-$ T cells (Figure 5J) and expressed TNF-α (Figure 5K). However, colonic $CCL5^+$ T cells did not express the cytokines interferon γ (IFNγ) and IL-10 (Figure 5K), nor the neutrophil-recruiting chemokines CXCL1, CCL2, and CCL3 (Figure 5K).[22] Interestingly, Il-$3^{-/-}$ and $Cd131^{-/-}$ mice showed reduced $CCL5^+$ T cell numbers in the colon compared with WT controls (Figures 5I and S4C), and severe combined immunodeficiency (SCID) mice exhibited reduced *Ccl5* mRNA expression (Figure 5L) and neutrophil numbers (Figure 5M) in the colon 1 day after the onset of DSS-induced colitis. These data suggest that CCL5-producing T cells promote the IL-3-dependent recruitment of neutrophils into the colon during DSS-induced colitis. Interestingly, the *ex vivo* stimulation of colonic cells from naive WT mice with IL-3 did not induce *Ccl5* mRNA expression

(Figure 5N). As observed in humans (Figure 1F), no expression of CD123 was detected at the surface of colonic T cells from naive WT mice (Figure S4D). This suggested that the reduced number of $CCL5^+$ T cells observed in the colon of Il-$3^{-/-}$ mice resulted most likely from reduced $CCL5^+$ T cell recruitment into the colon rather than from a reduced CCL5 expression by colonic T cells. Interestingly, we observed that the *ex vivo* stimulation of purified colonic immune cells from WT mice with IL-3 resulted in higher *Ccl20* expression (Figure 5N), a chemokine described to promote T cell recruitment.[23–25] By contrast, colonic immune cells obtained from naive Il-$3^{-/-}$ mice exhibited reduced expression of *Ccl20* compared with naive WT controls (Figure 5O). In addition, $CCL5^+$ T cells showed increased expression of CCR6, the receptor for CCL20, at their surface compared with $CCL5^-$ T cells (Figure 5P), and neutralization of CCL20 by the administration of anti-CCL20 antibodies resulted in reduced $CCL5^+$ T cell numbers in the colon 1 day after the onset of DSS-induced colitis (Figure 5Q) as well as reduced colonic neutrophil numbers (Figure 5R) and pronounced weight loss (Figure 5S). Thus, our data reveal that the early IL-3-dependent influx of neutrophils into the colon requires the recruitment of PD-1^{high} LAG-3^{high} CCR6^{high} TNFα$^+$ $CCL5^+$ T cells by CCL20.

IL-3 is produced by MSC-like cells in colon

IL-3 was recently described to be produced by astrocytes,[10] indicating that both hematopoietic and non-hematopoietic cells can produce IL-3. To identify the source of protective IL-3 during
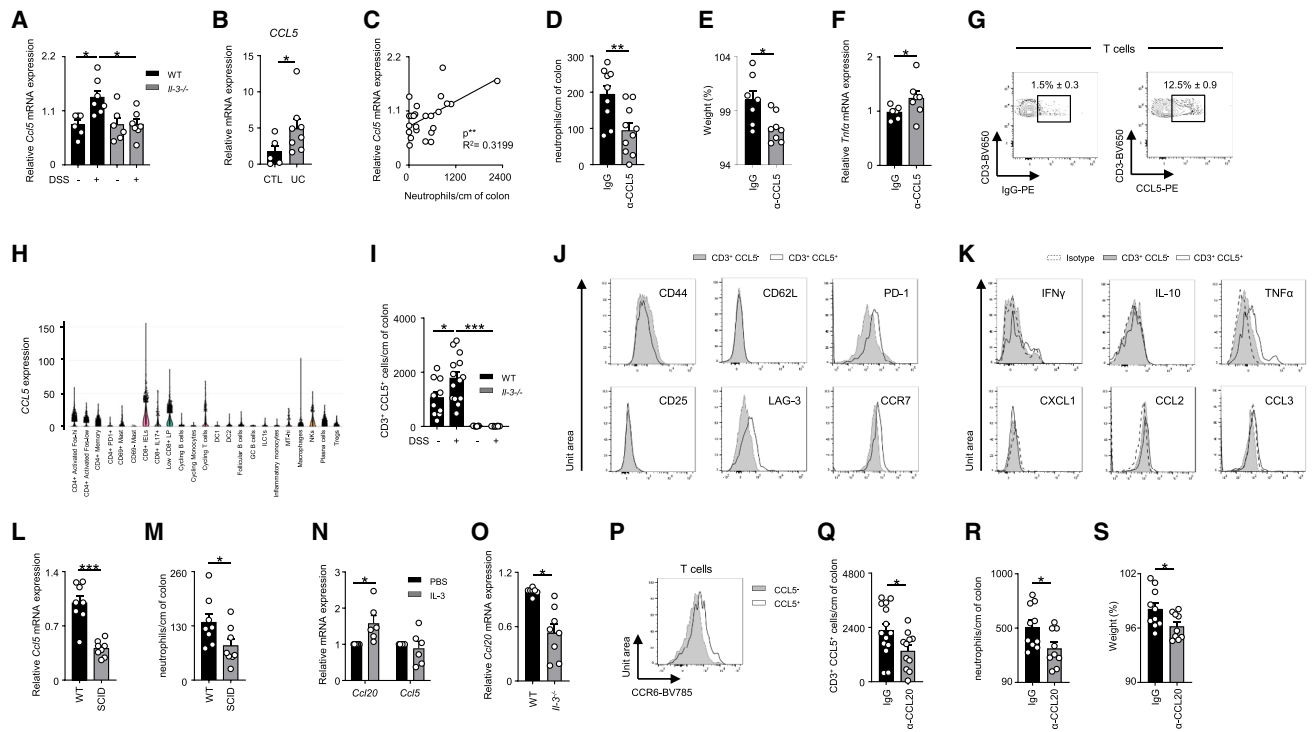
Figure 5. IL-3 induces early neutrophil influx into the colon in a CCL5-expressing CD3⁺ T cells and CCL20-dependent manner

(A) Relative *Ccl5* mRNA expression in colon tissues of naive as well as for 24 h DSS-treated WT and *Il-3*⁻/⁻ mice t (n = 6–7 per group).

(B) Relative mRNA expression of *CCL5* in control colon and in the colon of patients with UC (n = 5–8 per group).

(C) Correlation between *Ccl5* mRNA expression and the number of neutrophils in colon 24 h after the onset of colitis. Data from WT and *Il-3*⁻/⁻ mice were pooled (n = 24 per group) and analyzed by Pearson correlation test.

(D–F) WT mice received intravenous injection of anti-CCL5 antibodies or isotype controls at the onset of colitis. (D) Enumeration of neutrophils in colon (n = 9–10 per group). (E) Loss of weight (n = 7–8 per group). (F) Relative *Tnfα* mRNA expression in colon (n = 6–7 per group).

(G) Representative dot plots and cumulative percentages of CCL5⁺ cells among colonic T cells of WT mice 24 h after DSS administration (n = 5 per group).

(H) mRNA expression of *CCL5* in immune cells from colon of patients with UC. Data came from a retrospective analysis of single-cell RNA-seq atlas of colon biopsies from patients with UC.[21]

(I) Enumeration of CCL5⁺ CD3⁺ T cells in the colon of WT and *Il-3*⁻/⁻ mice 24 h after DSS administration (n = 7–14 per group).

(J) Representative histogram of CD44, CD25, CD62L, PD-1, LAG-3, and CCR7 expressed at the surface of CD3⁺ CCL5⁺ and CD3⁺ CCL5⁻ T cells from colon of WT naive mice (n = 5 per group).

(K) Representative histogram of IFNγ, IL-10, TNF-α, CXCL1, CCL2, and CCL3 expressed at the surface of CD3⁺ CCL5⁺ and CD3⁺ CCL5− T cells from colon of WT naive mice (n = 5 per group).

(L and M) Relative *Ccl5* mRNA expression (L) and neutrophil enumeration (M) in colon of WT and SCID mice 24 h after DSS administration (n = 8 per group).

(N) Relative mRNA expression of *Ccl20* and *Ccl5* in colon of WT mice 24 h after *ex vivo* stimulation with PBS or IL-3 (n = 6).

(O) Relative *Ccl20* mRNA expression in colon of naive WT and *Il-3*⁻/⁻ mice (n = 7–8 per group).

(P) Representative histogram of CCR6 expressed at the surface of CD3⁺ CCL5⁺ and CD3⁺ CCL5⁻ T cells from naive mice (n = 5 per group).

(Q–S) WT mice received either an intravenous injection of anti-CCL20 antibodies or its isotype control just before DSS administration. Mice were sacrificed 24 h later. (Q) Enumeration of CCL5⁺ CD3⁺ T cells in colon tissues (n = 11–14 per group). (R) Enumeration of neutrophils in colon tissues (n = 9–10 per group). (S) Loss of weight (n = 9–10 per group).

(A, C, F, L, N, and O) The expression level was arbitrarily set to 1 for one sample from the control group, and the values for the other samples were calculated relatively to this reference.

Data are pooled data from at least 2 independent experiments. Data represent mean ± SEM and were analyzed by the two-tailed unpaired (B, D–F, L, M, O, and Q–S) or paired (N) t test or the Tukey's multiple comparison test (A and I). *p < 0.05; **p < 0.01; ***p < 0.001.

DSS-induced colitis, we generated BM chimeric mice in which either hematopoietic (IL-3/WT) or non-hematopoietic cells (WT/IL-3) were unable to produce IL-3, as well as their corresponding controls (WT/WT and IL-3/IL-3). Remarkably, only mice with a non-hematopoietic IL-3 deficiency exhibited the same reduced survival (Figure 6A) and weight loss (Figure 6B) as IL-3/IL-3 mice following DSS-induced colitis. Flow cytometry analysis characterized the IL-3-expressing population as CD45⁻ CD31⁻ CD326⁻/low gp38⁺ Sca-1⁻ VCAM⁻ ICAM⁺, cells that were present in colon at steady state and following DSS-induced colitis (Figures 6C and 6D). Based on CD73 and CD105 expression, two markers of mesenchymal stem cells (MSC), we identified three distinct populations: CD73⁺ CD105⁺ cells, CD73⁺ CD105⁻ cells, and CD73⁻ CD105⁻ cells (Figure 6E). The depletion of IL-3 only in non-hematopoietic cells resulted in increased plasma TNF-α levels (Figure 6F) and in a reduced number of
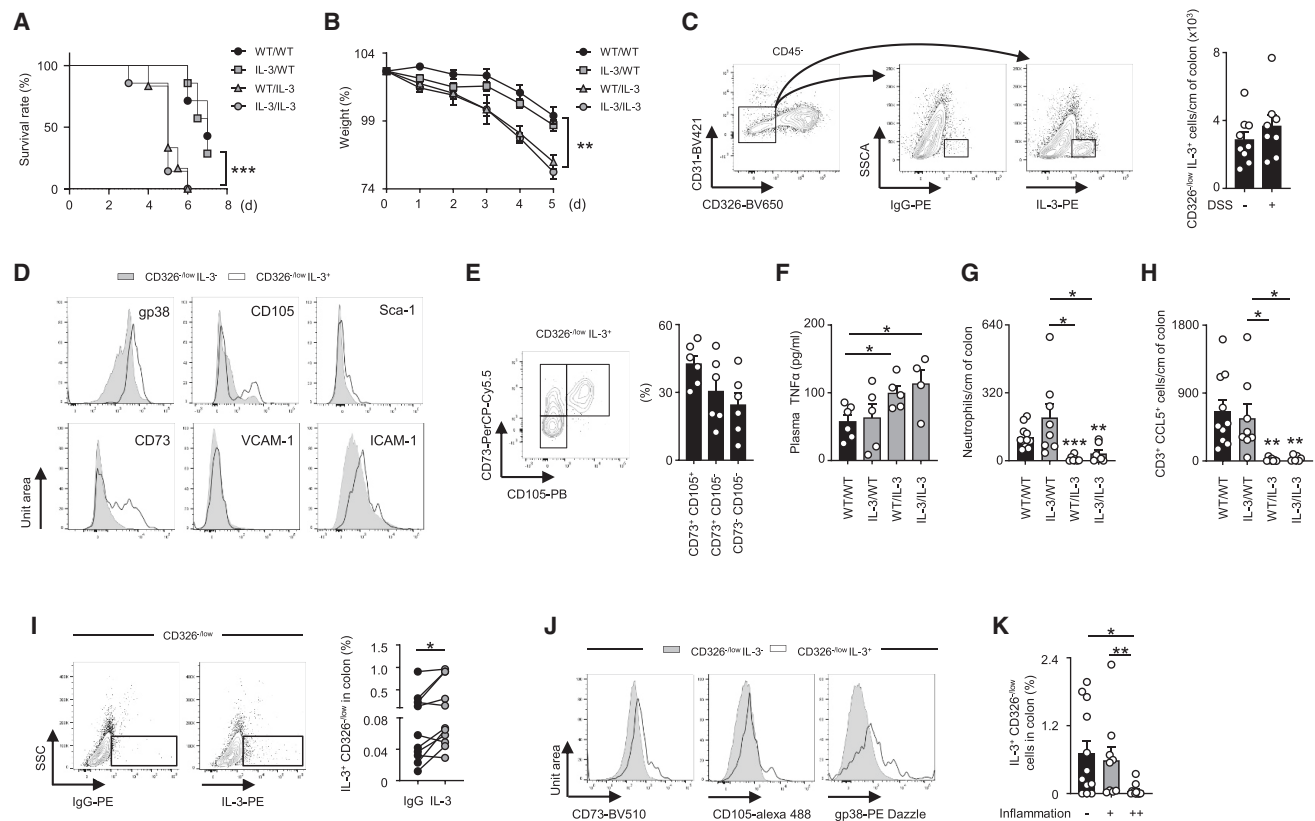
Figure 6. IL-3-expressing MSC-like cells limit the development of experimental colitis in mice

(A and B) Survival (A) and weight loss (B) in WT/WT, IL-3/WT, WT/IL-3, and IL-3/IL-3 chimeric mice upon DSS treatment (n = 6–7 per group). Data were analyzed by log rank (Mantel-Cox) test (A).

(C) Gating strategy and enumeration of non-hematopoietic cells expressing IL-3 in the colon of WT mice treated or not during 24 h with DSS (n = 8–9 per group).

(D) Representative histogram of markers expressed at the surface of IL-3$^+$ CD326$^{-/low}$ or IL-3$^-$ CD326$^{-/low}$ cells in the colon of naive WT mice (n = 6 per group).

(E) Representative dot plots and percentage of CD73$^+$CD105$^+$, CD73$^+$CD105^{-+} and CD73$^-$CD105$^-$ cells in IL-3$^+$ CD326$^{-/low}$ cells in the colon of naive WT mice (n = 6 per group).

(F–H) WT/WT, IL-3/WT, WT/IL-3, and IL-3/IL-3 chimera mice were treated for 24 h with DSS. (F) Levels of plasma TNF-α (n = 4–6 per group). (G) Enumeration of neutrophils in colon (n = 7–11). (H) Enumeration of CCL5$^+$ CD3$^+$ T cells in colon (n = 6–10 per group).

(I) Representative dot plots and percentage of CD326$^{-/low}$ cells expressing IL-3 in the colon of patients with UC (n = 11 per group).

(J) Representative histogram of markers expressed at the surface of IL-3$^+$ CD326$^{-/low}$ or IL-3$^-$ CD326$^{-/low}$ cells (n = 11 per group).

(K) Percentage of IL-3$^+$ CD326$^{-/low}$ cells in control colon (−) or in colon from the same UC patient with either low (+) or high (++) levels of inflammation (n = 9–12 per group).

Data are pooled data from at least 2 independent experiments. Data represent mean ± SEM and were analyzed by the Dunnett's multiple comparisons test (B) or the two-tailed unpaired t test (C–K). *p < 0.05; **p < 0.01.

---

neutrophils (Figure 6G) and CCL5$^+$ T cells (Figure 6H) in the colon after 1 day of DSS colitis, similar to what was observed in *Il-3*$^{-/-}$ mice (Figure 2). In humans, we found a similar IL-3-producing CD45$^-$ CD31$^-$ CD326^{low} gp38$^+$ population in the colon of patients with UC (Figures 6I and 6J). Interestingly, the percentage of this population was reduced in the colon with high inflammation (Figure 6K). Altogether, these data suggest that early protection against colitis requires local IL-3 production by cells harboring an MSC phenotype.

IL-3 controls extramedullary hematopoiesis during colitis

Previous studies reported that IL-3 could sustain extramedullary hematopoiesis in spleen.[26] One day after the induction of colitis,

we observed that WT mice showed increased spleen weight (Figure S5A) and increased numbers of neutrophils (Figure S5B), CD45$^+$ Lin$^-$ cKit$^+$ hematopoietic stem and progenitor cells (HSPCs) (Figure S5C), and proliferative Ki-67$^+$ HSPCs (Figure S5D) in the spleen, whereas no difference was observed in BM or in the spleen of *Il-3*$^{-/-}$ mice (Figures S5A–S5D). Likewise, recombinant IL-3 administration in *Il-3*$^{-/-}$ mice resulted in higher spleen weight (Figure S5E) and increased numbers of neutrophils (Figure S5F) and HSPCs (Figure S5G) compared with controls upon DSS-induced colitis, suggesting that IL-3 promotes extramedullary hematopoiesis in the spleen during colitis. Interestingly, mice with a hematopoietic or non-hematopoietic *Il-3* deficiency exhibited reduced spleen weight (Figure S5H) as well as neutrophil (Figure S5I) and HSPC numbers (Figure S5J).
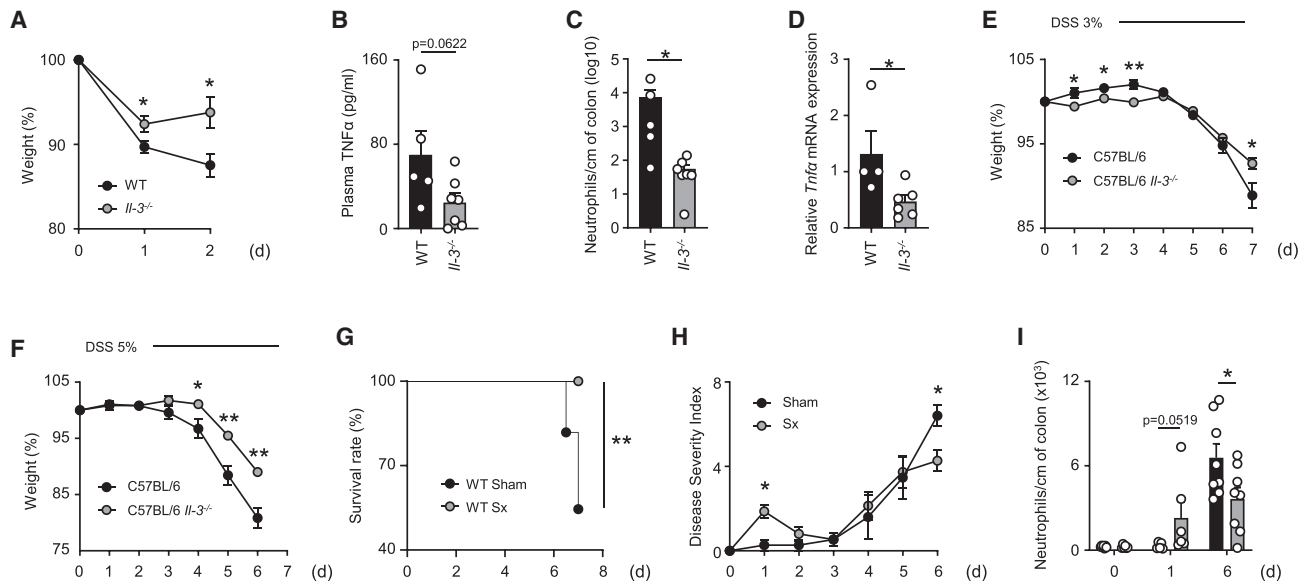
Figure 7. IL-3 amplifies inflammation during acute colitis

(A) Comparison of weight loss in WT and $Il-3^{-/-}$ mice 48 h after intra-rectal administration of oxazolone (n = 9–10 per group).

(B) Levels of plasma TNF-α in WT and $Il-3^{-/-}$ mice 48 h after intra-rectal administration of oxazolone (n = 5–7 per group).

(C) Enumeration of neutrophils in colon of WT and $Il-3^{-/-}$ mice 48 h after intra-rectal administration of oxazolone (n = 5–7 per group).

(D) Relative $Tnf\alpha$ mRNA expression in colon of WT and $Il-3^{-/-}$ mice 48 h after intra-rectal administration of oxazolone; the expression level was arbitrarily set to 1 for one sample from the WT group, and the values for the other samples were calculated relatively to this reference (n = 4–6 per group).

(E and F) Comparison of weight loss in C57BL/6 WT and $Il-3^{-/-}$ mice upon 3% (E) or 5% (F) DSS treatment (n = 8–11 per group).

(G) Survival curve of sham or splenectomized WT mice upon DSS application (n = 11–12 per group). Data were analyzed by log rank (Mantel-Cox) test.

(H) Severity index of sham or splenectomized WT mice following DSS colitis induction (n = 5 per group).

(I) Enumeration of neutrophils in colon of sham or splenectomized (Sx) WT mice 0, 1, and 6 days after DSS administration (n = 8 per group).

Data represent mean ± SEM and were analyzed by the two-tailed unpaired t test (A–I). *p < 0.05; **p < 0.01; ***p < 0.001.

Although we were not able to detect splenic non-hematopoietic cells expressing IL-3, we observed an increase of IL-3-expressing innate response activator (IRA) B cells in the spleen over the time of colitis (Figures S5K and S5L). Collectively, our data suggest that IL-3-mediated extramedullary splenic hematopoiesis sustains neutrophil mobilization during the early phase of colitis.

Early neutrophil and CCL5⁺ T cell recruitment into the colon requires STAT5 signaling

Biological activities of IL-3 require mainly STAT5 and STAT3.[27] We therefore investigated which of these two transcription factors orchestrates the action of IL-3 during colitis. Mice treated with a chemical inhibitor of STAT5 exhibited pronounced weight loss (Figure S6A) as well as reduced neutrophil and CCL5⁺ T cell numbers (Figures S6B and S6C) in the colon 1 day after the onset of DSS-induced colitis, whereas mice treated with a chemical inhibitor of STAT3 showed an increased neutrophil number in the colon (Figure S6B) after 1 day of DSS-induced colitis but did not exhibit any difference in weight loss and colonic CCL5⁺ T cell number compared with controls (Figures S6A and S6C). Thus, our results show that only mice in which STAT5 signaling is inhibited exhibited the same phenotype as in $Il-3^{-/-}$ mice, suggesting that the early protective effect of IL-3 during DSS-induced colitis is mediated by STAT5. In addition, STAT5 inhibition led to a reduction in the number of neutrophils and HSPCs in the spleen (Figures S6D and S6E) 24 h after the onset of DSS-

induced colitis, while STAT3 inhibition only led to reduced HSPC number (Figures S6D and S6E), suggesting that extramedullary splenic hematopoiesis during DSS-induced colitis is mainly associated with STAT5. Collectively, those data suggest that STAT5 orchestrates the main activities of IL-3 in DSS-induced colitis.

IL-3 amplifies inflammation during acute colitis

IL-3 was previously reported to amplify the acute phase of sepsis, resulting in increased mortality.[9] Remarkably, our present data showed that IL-3 limited the early development of colitis by enhancing the recruitment of splenic neutrophils into the colon. However, disease severity as well as intestinal inflammation were comparable at day 7 between BALB/c WT and $Il-3^{-/-}$ mice upon DSS administration (Figures 2C–2E and 2G). In addition, colon $IL-3$ mRNA expression correlated with disease severity in patients with UC (Figure 1C). Thus, these results suggested that IL-3 might modulate intestinal inflammation during the acute phase of colitis as well. To test this hypothesis, mice were treated with oxazolone, a haptenating agent inducing severe inflammation of the mucosa.[17] Upon oxazolone, $Il-3^{-/-}$ mice exhibited reduced weight loss compared with controls (Figure 7A). In addition, $Il-3^{-/-}$ mice displayed reduced plasma TNF-α levels (Figure 7B) as well as reduced neutrophil numbers (Figure 7C) and reduced $Tnf\alpha$ mRNA expression in the colon (Figure 7D) 48 h after intra-rectal administration of oxazolone

compared with controls. To exclude the possibility that the difference observed between DSS- and oxazolone-induced colitis was related to the very different nature and pathogenesis of the two models, we induced colitis in C57BL/6 and *Il-3*$^{-/-}$ C57BL/6 mice, the background described to be more susceptible to DSS-induced colitis,[28] using different DSS percentages (3% vs. 5%). As observed in the BALB/c background, the deletion of *Il-3* in C57BL/6 mice resulted in pronounced weight loss at the onset of colitis induced by 3% of DSS (Figure 7E). However, *Il-3*$^{-/-}$ C57BL/6 mice displayed reduced weight loss compared with controls after 7 days of 3% of DSS (Figure 7E), suggesting a detrimental role of IL-3 during severe DSS-induced colitis. Indeed, *Il-3*$^{-/-}$ C57BL/6 mice treated with 5% of DSS showed significant reduced weight loss from day 4 compared with WT C57BL/6 mice (Figure 7F). Thus, our results show that IL-3 also increases colitis severity during acute intestinal inflammation. Interestingly, IL-3 was described to fuel the cytokine storm during sepsis by inducing myelopoiesis.[9] Since IL-3 induced extramedullary splenic hematopoiesis during colitis (Figures S7A and S7B) and promoted the recruitment of splenic neutrophils into the colon (Figure 3), we wondered whether the detrimental effect of IL-3 during acute colitis was associated with the spleen. The ablation of the spleen in WT mice resulted in increased survival upon DSS administration (Figure 7G). By contrast, no differences were observed between sham and Sx *Il-3*$^{-/-}$ mice (Figure S7C), suggesting that IL-3 contributed to the detrimental effect of the spleen during acute colitis. Remarkably, we observed that the spleen has a dual role during colitis. Indeed, Sx WT mice exhibited increased weight loss (Figure 3C) as well as increased disease severity (Figure 7H) and neutrophil number in the colon (Figures 3E and 7I) after 1 day of DSS-induced colitis compared with control mice, indicating a protective role of the spleen at the onset of the disease. However, the spleen has a detrimental role during severe colitis as shown by the reduced disease severity after 6 days of DSS-induced colitis in Sx mice (Figure 7H) and the reduced neutrophil number (Figure 7I) after 6 days of DSS. Collectively, our data suggest that IL-3 and the spleen are important orchestrators of intestinal inflammation during colitis.

DISCUSSION

In our study, we showed that IL-3 has a dual role in colitis, which seems to depend on the intensity of the inflammation. At the onset of the disease, IL-3 has a beneficial role by promoting the recruitment of splenic neutrophils with high microbicidal capability into the colon, whereas IL-3 has a detrimental effect during severe colitis by amplifying intestinal inflammation. A similar phenomenon was already described for type I IFNs. Indeed, type I IFNs are critical for early immune responses against acute lymphocytic choriomeningitis virus (LCMV) infections.[29] However, blockade of type I IFN signaling reduced the immune suppression associated with the persistent infection, resulting in better clearance of the virus.[30,31] Furthermore, such opposite effects of IL-3 have already been described during cerebral inflammation. Whereas IL-3 limits Alzheimer's disease by programming microglia,[10] IL-3 promotes the development of experimental autoimmune encephalitis by increasing the recruit-

ment of leukocytes into the brain.[32] Thus, this study deepens the knowledge that IL-3 is a key orchestrator of inflammation.

Our study showed that IL-3 limits the development of colitis by promoting the recruitment of splenic neutrophils into the colon. So far, the contribution of the spleen in IBDs has remained elusive. In mice, it was reported that the development of DSS-induced colitis was either associated with a reduced, an increased, or an unaltered spleen weight.[33,34] In humans, patients with relapsing but not quiescent UC showed significantly smaller spleens than controls.[35] Likewise, small spleen size was associated with pre-surgical disease complications as well as surgical site infections in patients with IBD,[36] suggesting that a reduced spleen size during colitis may have detrimental effects. However, the ablation of the spleen in mice improved disease symptoms of DSS-induced colitis,[37] which suggests that the putative protective role of the spleen is either possibly associated with the level of inflammation or to a specific subset of splenic leukocytes such as neutrophils. In support of this, the adoptive transfer of splenic Gr1$^+$CD11b$^+$ cells purified during the resolution phase of colitis resulted in an ameliorated course of DSS-induced colitis through efficient colonic mucosal healing.[38] Neutrophils are the first immune cells that migrate toward the colon to protect from invading pathogens. Neutrophils have therefore a large arsenal to fight against pathogens.[15] Our data revealed that splenic neutrophils had higher microbicidal abilities than neutrophils from BM, indicating that splenic neutrophils are better equipped to protect against invading pathogens. Our study confirms a previous single-cell transcriptome profiling study showing increased maturity of neutrophils from the spleen compared with mature neutrophils from BM[19] and suggests that splenic neutrophils, or their progenitors, might receive microenvironmental education signals that are specific to the spleen. Thus, our study highlights the ability of the body to mobilize a reservoir of specialized splenic neutrophils during colitis. Harnessing this reservoir might therefore provide an advantage to the host for early bacteria eradication. Whether this phenomenon is specific to IBDs will require further investigation.

We detected IL-3 expression in the colon in cells harboring an MSC phenotype. MSCs are cells with immune-suppressive activity that are used in a wide diversity of cell therapy protocols for the treatment of inflammatory disorders such as IBDs.[4] The presence of these IL-3$^+$ cells in the colon at steady state and the expression of the receptor for IL-3 by colonic epithelial cells suggest that IL-3 might contribute to mucosal homeostasis by directly modulating the function of epithelial cells. This is strengthened by the description that epithelial cells are a major source of CCL20,[39] a cytokine induced by IL-3 in the colon. Furthermore, it was previously described that IL-3 attenuated collagen-induced arthritis by modulating the development of Foxp3$^+$ regulatory T cells.[13] Considering the importance of regulatory T cells in IBDs,[40] we cannot exclude that IL-3 may also protect by improving the regulatory T cell-associated immunosuppressive immunity.

Finally, we observed that IL-3 induces extramedullary hematopoiesis (EMH) in spleen during colitis. The spleen is an important EMH site during inflammation as shown by the high numbers of undifferentiated monocytes residing in the spleen, outnumbering their equivalent in the blood,[41] and by the accumulation of

progenitor cells during inflammation.[42] The role of EMH is to supplement the hematopoietic function of the BM in order to produce enough phagocytes to sustain the immune response or to increase ectopic erythropoiesis during hypoxia.[43] However, an excessive or prolonged EMH may amplify inflammatory diseases.[44] The ability of IL-3 to stimulate splenic EMH during IBDs might then become detrimental during acute colitis by fueling the inflammatory immune response as seen in sepsis,[9] which might explain the reduced disease symptoms observed in Sx mice during acute colitis. Our data revealed also that IL-3 promoted the recruitment of CCL5+ PD-1high LAG-3high T cells into the colon. LAG-3 and PD-1 expression were previously described on activated T cells in the inflamed colonic mucosa from patients with active UC and from mice upon azoxymethane (AOM)/DSS treatment.[45,46] As their cell numbers positively correlate with mucosal inflammation and disease activity, it is also possible that IL-3 potentiates inflammation during acute colitis by promoting the recruitment of these CCL5+ PD-1high LAG-3high T cells into the colon.

Altogether, our results support the hypothesis that IL-3 orchestrates intestinal inflammation during IBDs. Targeting IL-3 signaling may therefore have potential as a novel therapeutic approach. The prophylactic treatment with recombinant IL-3 might reduce the risk of relapse for patients with inactive UC by limiting the development of the disease. By contrast, the administration of antagonists for IL-3 or CD123 might protect patients with active UC by reducing intestinal inflammation.

Limitations of the study

Although we clearly demonstrated that IL-3 protects at the onset of DSS-induced colitis by promoting the early recruitment of splenic neutrophils in mice, it was not possible to extend this effect in humans. As well, we cannot exclude that the protective effect of IL-3 at the onset of colitis involved other mechanisms considering that (1) IL-3 is expressed at steady state and (2) many cells express the IL-3 receptor in the colon. Finally, it is difficult to draw conclusions regarding the role of splenic neutrophils during acute colitis considering that splenectomy can have many effects that are not mediated by neutrophils.

STAR★METHODS

Detailed methods are provided in the online version of this paper and include the following:

- KEY RESOURCES TABLE
- RESOURCE AVAILABILITY
  - Lead contact
  - Materials availability
  - Data and code availability
- EXPERIMENTAL MODEL AND STUDY PARTICIPANT DETAILS
  - Animals
  - Disease severity index
  - Mouse treatment
  - Human
- METHOD DETAILS
  - Murine leukocyte isolation
  - Human blood and tissue samples and leukocyte isolation
  - *Ex vivo* colon stimulation by IL-3
  - Chemotaxis assays
  - Mixed bone-marrow chimera
  - Histology
  - Immunohistochemistry
  - RNA-seq
  - Neutrophil function assays
  - Quantitative RT-PCR
  - Cytokine detection
  - Flow cytometry
- QUANTIFICATION AND STATISTICAL ANALYSIS

AUTHOR CONTRIBUTIONS

A.B. conceived the project, conceptualized, designed, and conducted experiments, collected, analyzed, and interpreted data, designed figures, and wrote the manuscript; A.M., B.K., K.G., J.S., B.N., E.N., M.S., J.M., and L.E.M. conducted experiments and collected, analyzed, and interpreted data; A.M., M.B., R.G., and G.F.W. provided clinical samples, protocols, or reagents and collected data; K.G., J.M., and K.S. performed and analyzed RNA-seq; G.F.W. conceived the project, conceptualized and designed experiments, interpreted data, and wrote the manuscript; all of the authors critically revised the manuscript for important intellectual content.

REFERENCES

1. Burisch, J., Jess, T., Martinato, M., and Lakatos, P.L.; ECCO -EpiCom (2013). The burden of inflammatory bowel disease in Europe. J. Crohns Colitis 7, 322–337.

2. Neurath, M.F. (2014). Cytokines in inflammatory bowel disease. Nat. Rev. Immunol. 14, 329–342.

3. Abraham, C., and Cho, J.H. (2009). Inflammatory bowel disease. N. Engl. J. Med. 361, 2066–2078.

4. Markovic, B.S., Kanjevac, T., Harrell, C.R., Gazdic, M., Fellabaum, C., Arsenijevic, N., and Volarevic, V. (2018). Molecular and cellular mechanisms

involved in mesenchymal stem cell-based therapy of inflammatory bowel diseases. Stem Cell Rev. Rep. *14*, 153–165.

5. Gisbert, J.P., Marín, A.C., and Chaparro, M. (2016). The risk of relapse after anti-TNF discontinuation in inflammatory bowel disease: systematic review and meta-analysis. Am. J. Gastroenterol. *111*, 632–647.

6. Niemeyer, C.M., Sieff, C.A., Mathey-Prevot, B., Wimperis, J.Z., Bierer, B.E., Clark, S.C., and Nathan, D.G. (1989). Expression of human interleukin-3 (multi-CSF) is restricted to human lymphocytes and T-cell tumor lines. Blood *73*, 945–951.

7. Lorentz, A., Schwengberg, S., Sellge, G., Manns, M.P., and Bischoff, S.C. (2000). Human intestinal mast cells are capable of producing different cytokine profiles: role of IgE receptor cross-linking and IL-4. J. Immunol. *164*, 43–48.

8. Ishizuka, T., Okayama, Y., Kobayashi, H., and Mori, M. (1999). Interleukin-3 production by mast cells from human lung. Inflammation *23*, 25–35.

9. Weber, G.F., Chousterman, B.G., He, S., Fenn, A.M., Nairz, M., Anzai, A., Brenner, T., Uhle, F., Iwamoto, Y., Robbins, C.S., et al. (2015). Interleukin-3 amplifies acute inflammation and is a potential therapeutic target in sepsis. Science *347*, 1260–1265.

10. McAlpine, C.S., Park, J., Griciuc, A., Kim, E., Choi, S.H., Iwamoto, Y., Kiss, M.G., Christie, K.A., Vinegoni, C., Poller, W.C., et al. (2021). Astrocytic interleukin-3 programs microglia and limits Alzheimer's disease. Nature *595*, 701–706.

11. Bénard, A., Jacobsen, A., Brunner, M., Krautz, C., Klösch, B., Swierzy, I., Naschberger, E., Podolska, M.J., Kouhestani, D., David, P., et al. (2021). Interleukin-3 is a predictive marker for severity and outcome during SARS-CoV-2 infections. Nat. Commun. *12*, 1112.

12. Anzai, A., Mindur, J.E., Halle, L., Sano, S., Choi, J.L., He, S., McAlpine, C.S., Chan, C.T., Kahles, F., Valet, C., et al. (2019). Self-reactive CD4(+) IL-3(+) T cells amplify autoimmune inflammation in myocarditis by inciting monocyte chemotaxis. J. Exp. Med. *216*, 369–383.

13. Srivastava, R.K., Tomar, G.B., Barhanpurkar, A.P., Gupta, N., Pote, S.T., Mishra, G.C., and Wani, M.R. (2011). IL-3 attenuates collagen-induced arthritis by modulating the development of Foxp3+ regulatory T cells. J. Immunol. *186*, 2262–2272.

14. Ligumsky, M., Kuperstein, V., Nechushtan, H., Zhang, Z., and Razin, E. (1997). Analysis of cytokine profile in human colonic mucosal Fc epsilonRI-positive cells by single cell PCR: inhibition of IL-3 expression in steroid-treated IBD patients. FEBS Lett. *413*, 436–440.

15. Kolaczkowska, E., and Kubes, P. (2013). Neutrophil recruitment and function in health and inflammation. Nat. Rev. Immunol. *13*, 159–175.

16. Fournier, B.M., and Parkos, C.A. (2012). The role of neutrophils during intestinal inflammation. Mucosal Immunol. *5*, 354–366.

17. Kiesler, P., Fuss, I.J., and Strober, W. (2015). Experimental models of inflammatory bowel diseases. Cell. Mol. Gastroenterol. Hepatol. *1*, 154–170.

18. Capucetti, A., Albano, F., and Bonecchi, R. (2020). Multiple roles for chemokines in neutrophil biology. Front. Immunol. *11*, 1259.

19. Xie, X., Shi, Q., Wu, P., Zhang, X., Kambara, H., Su, J., Yu, H., Park, S.Y., Guo, R., Ren, Q., et al. (2020). Single-cell transcriptome profiling reveals neutrophil heterogeneity in homeostasis and infection. Nat. Immunol. *21*, 1119–1133.

20. Hwaiz, R., Rahman, M., Syk, I., Zhang, E., and Thorlacius, H. (2015). Rac1-dependent secretion of platelet-derived CCL5 regulates neutrophil recruitment via activation of alveolar macrophages in septic lung injury. J. Leukoc. Biol. *97*, 975–984.

21. Smillie, C.S., Biton, M., Ordovas-Montanes, J., Sullivan, K.M., Burgin, G., Graham, D.B., Herbst, R.H., Rogel, N., Slyper, M., Waldman, J., et al. (2019). Intra- and inter-cellular rewiring of the human colon during ulcerative colitis. Cell *178*, 714–730.e22.

22. Metzemaekers, M., Gouwy, M., and Proost, P. (2020). Neutrophil chemoattractant receptors in health and disease: double-edged swords. Cell. Mol. Immunol. *17*, 433–450.

23. Liao, F., Rabin, R.L., Smith, C.S., Sharma, G., Nutman, T.B., and Farber, J.M. (1999). CC-chemokine receptor 6 is expressed on diverse memory subsets of T cells and determines responsiveness to macrophage inflammatory protein 3 alpha. J. Immunol. *162*, 186–194.

24. Wang, C., Kang, S.G., Lee, J., Sun, Z., and Kim, C.H. (2009). The roles of CCR6 in migration of Th17 cells and regulation of effector T-cell balance in the gut. Mucosal Immunol. *2*, 173–183.

25. Kitamura, K., Farber, J.M., and Kelsall, B.L. (2010). CCR6 marks regulatory T cells as a colon-tropic, IL-10-producing phenotype. J. Immunol. *185*, 3295–3304.

26. Robbins, C.S., Chudnovskiy, A., Rauch, P.J., Figueiredo, J.L., Iwamoto, Y., Gorbatov, R., Etzrodt, M., Weber, G.F., Ueno, T., van Rooijen, N., et al. (2012). Extramedullary hematopoiesis generates Ly-6C(high) monocytes that infiltrate atherosclerotic lesions. Circulation *125*, 364–374.

27. Nagata, Y., and Todokoro, K. (1996). Interleukin 3 activates not only JAK2 and STAT5, but also Tyk2, STAT1, and STAT3. Biochem. Biophys. Res. Commun. *221*, 785–789.

28. Yang, F., Wang, D., Li, Y., Sang, L., Zhu, J., Wang, J., Wei, B., Lu, C., and Sun, X. (2017). Th1/Th2 balance and Th17/treg-mediated immunity in relation to murine resistance to dextran sulfate-induced colitis. J. Immunol. Res. *2017*, 7047201.

29. Lee, A.J., and Ashkar, A.A. (2018). The dual nature of type I and type II interferons. Front. Immunol. *9*, 2061.

30. Teijaro, J.R., Ng, C., Lee, A.M., Sullivan, B.M., Sheehan, K.C.F., Welch, M., Schreiber, R.D., de la Torre, J.C., and Oldstone, M.B.A. (2013). Persistent LCMV infection is controlled by blockade of type I interferon signaling. Science *340*, 207–211.

31. Wilson, E.B., Yamada, D.H., Elsaesser, H., Herskovitz, J., Deng, J., Cheng, G., Aronow, B.J., Karp, C.L., and Brooks, D.G. (2013). Blockade of chronic type I interferon signaling to control persistent LCMV infection. Science *340*, 202–207.

32. Renner, K., Hellerbrand, S., Hermann, F., Riedhammer, C., Talke, Y., Schiechl, G., Rodriguez Gomez, M., Kutzi, S., Halbritter, D., Goebel, N., et al. (2016). IL-3 promotes the development of experimental autoimmune encephalitis. JCI Insight *1*, e87157.

33. Axelsson, L.G., Landström, E., and Bylund-Fellenius, A.C. (1998). Experimental colitis induced by dextran sulphate sodium in mice: beneficial effects of sulphasalazine and olsalazine. Aliment. Pharmacol. Ther. *12*, 925–934.

34. Morteau, O., Morham, S.G., Sellon, R., Dieleman, L.A., Langenbach, R., Smithies, O., and Sartor, R.B. (2000). Impaired mucosal defense to acute colonic injury in mice lacking cyclooxygenase-1 or cyclooxygenase-2. J. Clin. Invest. *105*, 469–478.

35. Muller, A.F., Cornford, E., and Toghill, P.J. (1993). Splenic function in inflammatory bowel disease: assessment by differential interference microscopy and splenic ultrasound. Q. J. Med. *86*, 333–340.

36. Pereira, J.L., Hughes, L.E., and Young, H.L. (1987). Spleen size in patients with inflammatory bowel disease. Does it have any clinical significance? Dis. Colon Rectum *30*, 403–409.

37. Krieglstein, C.F., Cerwinka, W.H., Laroux, F.S., Grisham, M.B., Schürmann, G., Brüwer, M., and Granger, D.N. (2001). Role of appendix and spleen in experimental colitis. J. Surg. Res. *101*, 166–175.

38. Zhang, R., Ito, S., Nishio, N., Cheng, Z., Suzuki, H., and Isobe, K.I. (2011). Dextran sulphate sodium increases splenic Gr1(+)CD11b(+) cells which accelerate recovery from colitis following intravenous transplantation. Clin. Exp. Immunol. *164*, 417–427.

39. Crane-Godreau, M.A., and Wira, C.R. (2004). Effect of Escherichia coli and Lactobacillus rhamnosus on macrophage inflammatory protein 3 alpha, tumor necrosis factor alpha, and transforming growth factor beta release by polarized rat uterine epithelial cells in culture. Infect. Immun. *72*, 1866–1873.

40. Clough, J.N., Omer, O.S., Tasker, S., Lord, G.M., and Irving, P.M. (2020). Regulatory T-cell therapy in Crohn's disease: challenges and advances. Gut *69*, 942–952.

41. Swirski, F.K., Nahrendorf, M., Etzrodt, M., Wildgruber, M., Cortez-Retamozo, V., Panizzi, P., Figueiredo, J.L., Kohler, R.H., Chudnovskiy, A., Waterman, P., et al. (2009). Identification of splenic reservoir monocytes and their deployment to inflammatory sites. Science *325*, 612–616.

42. Griseri, T., McKenzie, B.S., Schiering, C., and Powrie, F. (2012). Dysregulated hematopoietic stem and progenitor cell activity promotes interleukin-23-driven chronic intestinal inflammation. Immunity *37*, 1116–1129.

43. Kim, C.H. (2010). Homeostatic and pathogenic extramedullary hematopoiesis. Hematol. Res. Rev. *1*, 13–19.

44. Regan-Komito, D., Swann, J.W., Demetriou, P., Cohen, E.S., Horwood, N.J., Sansom, S.N., and Griseri, T. (2020). GM-CSF drives dysregulated hematopoietic stem cell activity and pathogenic extramedullary myelopoiesis in experimental spondyloarthritis. Nat. Commun. *11*, 155.

45. Slevin, S.M., Garner, L.C., Lahiff, C., Tan, M., Wang, L.M., Ferry, H., Greenaway, B., Lynch, K., Geremia, A., Hughes, S., et al. (2020). Lymphocyte activation gene (LAG)-3 is associated with mucosal inflammation and disease activity in ulcerative colitis. J. Crohns Colitis *14*, 1446–1461.

46. Yassin, M., Sadowska, Z., Djurhuus, D., Nielsen, B., Tougaard, P., Olsen, J., and Pedersen, A.E. (2019). Upregulation of PD-1 follows tumour development in the AOM/DSS model of inflammation-induced colorectal cancer in mice. Immunology *158*, 35–46.

47. Wirtz, S., Popp, V., Kindermann, M., Gerlach, K., Weigmann, B., Fichtner-Feigl, S., and Neurath, M.F. (2017). Chemically induced mouse models of acute and chronic intestinal inflammation. Nat. Protoc. *12*, 1295–1309.

48. Barthel, M., Hapfelmeier, S., Quintanilla-Martínez, L., Kremer, M., Rohde, M., Hogardt, M., Pfeffer, K., Rüssmann, H., and Hardt, W.D. (2003). Pretreatment of mice with streptomycin provides a Salmonella enterica serovar Typhimurium colitis model that allows analysis of both pathogen and host. Infect. Immun. *71*, 2839–2858.

49. Udden, S.M.N., Waliullah, S., Harris, M., and Zaki, H. (2017). The ex vivo colon organ culture and its use in antimicrobial host defense studies. J. Vis. Exp. *120*, 55347.

50. Brian B. BBMap Short Read Aligner, and Other Bioinformatic Tools. http://sourceforge.net/projects/bbmap/.

51. Sedlazeck, F.J., Rescheneder, P., and von Haeseler, A. (2013). NextGenMap: fast and accurate read mapping in highly polymorphic genomes. Bioinformatics *29*, 2790–2791.

52. Liao, Y., Smyth, G.K., and Shi, W. (2014). featureCounts: an efficient general purpose program for assigning sequence reads to genomic features. Bioinformatics *30*, 923–930.

53. Kucukural, A., Yukselen, O., Ozata, D.M., Moore, M.J., and Garber, M. (2019). DEBrowser: interactive differential expression analysis and visualization tool for count data. BMC Genom. *20*, 6.

54. Love, M.I., Huber, W., and Anders, S. (2014). Moderated estimation of fold change and dispersion for RNA-seq data with DESeq2. Genome Biol. *15*, 550.

55. Bénard, A., Cavaillès, P., Boué, J., Chapey, E., Bayry, J., Blanpied, C., Meyer, N., Lamant, L., Kaveri, S.V., Brousset, P., and Dietrich, G. (2010). mu-Opioid receptor is induced by IL-13 within lymph nodes from patients with Sezary syndrome. J. Invest. Dermatol. *130*, 1337–1344.

STAR★METHODS

KEY RESOURCES TABLE

REAGENT or RESOURCE	SOURCE	IDENTIFIER
Antibodies		
PE anti-mouse CD19	BD Biosciences	Cat# 553786; RRID:AB_395050
PE CF594 anti-mouse CD11b	BD Biosciences	Cat# 553311; RRID:AB_394775
PE anti-mouse CD11c	BD Biosciences	Cat# 553802; RRID:AB_395061
PE anti-mouse CD49b	BD Biosciences	Cat# 553858; RRID:AB_395094
PE anti-mouse CD90.2	BD Biosciences	Cat# 553006; RRID:AB_394545
PE anti-mouse B220	BD Biosciences	Cat# 553090; RRID:AB_394620
PE anti-mouse Ter119	BD Biosciences	Cat# 553673; RRID:AB_394986
PE anti-mouse CD127	Biolegend	Cat# 121112; RRID:AB_493509
PE anti-mouse Gr1	Biolegend	Cat# 108408; RRID:AB_313373
BV711 anti-mouse SCA-1	BD Biosciences	Cat# 563992; RRID:AB_2738529
BV605 anti-mouse c-Kit	Biolegend	Cat# 135121; RRID:AB_2562040
FITC anti-mouse CD34	BD Biosciences	Cat# 553733; RRID:AB_395017
BUV395 anti-mouse CD16/32	BD Biosciences	Cat# 740217; RRID:AB_2739965
PerCP-Cy5.5 anti-mouse CD115	Biolegend	Cat# 135526; RRID:AB_2566462
BV650 anti-mouse CD326	BD Biosciences	Cat# 740559; RRID:AB_2740260
FITC anti-mouse Ly6C	BD Biosciences	Cat# 553104; RRID:AB_394628
BUV737 anti-mouse CD11b	BD Biosciences	Cat# 612800; RRID:AB_2870127
BV711 anti-mouse MHCII	BD Biosciences	Cat# 563414; RRID:AB_2738191
BV510 anti-mouse F4/80	BD Biosciences	Cat# 743280; RRID:AB_2741398
BUV395 anti-mouse Ly6G	BD Biosciences	Cat# 563978; RRID:AB_2716852
BV421 anti-mouse CD19	BD Biosciences	Cat# 562701; RRID:AB_2737731
PerCP-Cy5.5 anti-mouse CD3	BD Biosciences	Cat# 560527; RRID:AB_1727463
PerCP-Cy5. 5 anti-mouse CD138	Biolegend	Cat# 142510; RRID:AB_2561601
BV786 anti-mouse CD45.2	BD Biosciences	Cat# 563686; RRID:AB_2738375
FITC anti-mouse CD43	BD Biosciences	Cat# 553270; RRID:AB_394747
BV650 anti-mouse IgM	BD Biosciences	Cat# 564027; RRID:AB_2738552
BV510 anti-mouse CD5	BD Biosciences	Cat# 563069; RRID:AB_2737986
BUV395 anti-mouse CD93	BD Biosciences	Cat# 740275; RRID:AB_2740015
BV650 anti-mouse CD3	BD Biosciences	Cat# 564378; RRID:AB_2738779
PE-Dazzle anti-mouse CD3	Biolegend	Cat# 100245; RRID:AB_2565882
FITC anti-mouse TCRβ	Biolegend	Cat# 109216; RRID:AB_493345
BV711 anti-mouse CD8	BD Biosciences	Cat# 563046; RRID:AB_2737972
BUV395 anti-mouse CD4	BD Biosciences	Cat# 565974; RRID:AB_2739427
BV421 anti-mouse TCRγδ	Biolegend	Cat# 118119; RRID:AB_10896753
Pacific Blue anti-mouse CD31	Biolegend	Cat# 102421; RRID:AB_10613457
PerCP-Cy5.5 anti-mouse CD73	Biolegend	Cat# 127213; RRID:AB_11219608
PE anti-mouse CCR1	Biolegend	Cat# 152507; RRID:AB_2800688
FITC anti-mouse CCR3	Biolegend	Cat# 144509; RRID:AB_2561608
PerCP-Cy5.5 anti-mouse CCR5	Biolegend	Cat# 107015; RRID:AB_2616985
BV786 anti-mouse CCR6	Biolegend	Cat# 129823; RRID:AB_2715923
PE-Dazzle anti-mouse CXCR4	Biolegend	Cat# 146513; RRID:AB_2563682
Pacific Blue anti-mouse CD62L	BD Biosciences	Cat# 562910; RRID:AB_2737885
PerCP-Cy5.5 anti-mouse PD-L1	Biolegend	Cat# 124333; RRID:AB_2629831

(Continued on next page)

Continued

REAGENT or RESOURCE	SOURCE	IDENTIFIER
BV711 anti-mouse CD64	Biolegend	Cat# 139311; RRID:AB_2563846
FITC anti-mouse gp38	Biolegend	Cat# 127415; RRID:AB_2629801
PerCP-Cy5.5 anti-mouse CD54	Biolegend	Cat# 116123; RRID:AB_2715951
BUV395 anti-mouse CD106	BD Biosciences	Cat# 745672; RRID:AB_2743162
Pacific Blue anti-mouse CD105	Biolegend	Cat# 120411; RRID:AB_1877185
PerCP-Cy5.5 anti-mouse CD44	Biolegend	Cat# 103035; RRID:AB_10639933
FITC anti-mouse CD25	Biolegend	Cat# 101907; RRID:AB_961210
PE-Dazzle anti-mouse CD223	Biolegend	Cat# 125223; RRID:AB_2572081
PerCP-Cy5.5 anti-mouse PD-1	Biolegend	Cat# 135207; RRID:AB_10550092
PE-Dazzle 594 anti-mouse CCR7	Biolegend	Cat# 120121; RRID:AB_2564316
PE anti-mouse CD123	Biolegend	Cat# 106005; RRID:AB_2124403
Rat IgG2a-PE	Biolegend	Cat# 400501; RRID:AB_326523
PE anti-mouse CCL5	Biolegend	Cat# 149103; RRID:AB_2564405
Mouse IgG2b-PE	Biolegend	Cat# 400311; RRID:AB_2894969
PE anti-mouse IL-3	BD Biosciences	Cat# 554383; RRID:AB_395358
Rat IgG1-PE	BD Biosciences	Cat# 554685; RRID:AB_395509
eFluor 450 anti-mouse IL-1β	ThermoFischer	Cat# 48-7114-80; RRID:AB_2574108
Rat IgG1- eFluor 450	ThermoFischer	Cat# 53-4301-80; RRID:AB_493962
PerCP-Cy5.5 anti-mouse TNFα	BD Biosciences	Cat# 560659; RRID:AB_1727580
Rat IgG1-PerCP Cy5.5	BD Biosciences	Cat# 560537; RRID:AB_1645667
BV650 anti-mouse IL-10	BD Biosciences	Cat# 564083; RRID:AB_2738583
Rat IgG2-BV650	Biolegend	Cat# 400651
BUV737 anti-mouse IFNγ	BD Biosciences	Cat# 612769; RRID:AB_2870098
Rat IgG2a- BUV737	BD Biosciences	Cat# 612760; RRID:AB_2870091
BV785 anti-mouse IL-17A	Biolegend	Cat# 506928; RRID:AB_2629787
Rat IgG1-BV785	Biolegend	Cat# 400443
Alexa Fluor 488 anti-mouse CXCL1	R&D Systems	Cat# IC4532G
Rabbit IgG- Alexa Fluor 488	R&D Systems	Cat# IC1051G; RRID:AB_2819362
Alexa Fluor 405 anti-mouse CCL2	R&D Systems	Cat# FAB4791V
Rat IgG2b- Alexa Fluor 405	R&D Systems	Cat# IC013V
Alexa Fluor 488 anti- mouse CCL3	R&D Systems	Cat# IC450G
Rat IgG2a-Alexa Fluor 488	R&D Systems	Cat# IC006G; RRID:AB_10890915
PE-Dazzle anti-mouse/human Ki-67	Biolegend	Cat# 652427; RRID:AB_2632695
BUV737 anti-human CD14	BD Biosciences	Cat# 612763; RRID:AB_2870094
BV421 anti-human CD15	Biolegend	Cat# 323039; RRID:AB_2566519
PerCP-Cy5.5 anti-human HLADR	BD Biosciences	Cat# 560652; RRID:AB_1727529
FITC anti-human CD16	Biolegend	Cat# 302005; RRID:AB_314205
PE anti-human CD64	Biolegend	Cat# 305007; RRID:AB_314491
BV711 anti-human CD11c	BD Biosciences	Cat# 563130; RRID:AB_2738019
BUV395 anti-human CD19	BD Biosciences	Cat# 563551; RRID:AB_2738274
BV786 anti-human CD45	BD Biosciences	Cat# 563716; RRID:AB_2716864
BV510 anti-human CD3	BD Biosciences	Cat# 563109; RRID:AB_2732053
BV650 anti-human CD326	Biolegend	Cat# 324225; RRID:AB_2562734
PE-CF594 anti-human CD123	BD Biosciences	Cat# 562391; RRID:AB_11153664
Mouse IgG2a-PE-CF594	BD Biosciences	Cat# 562306; RRID:AB_11153843
PerCP-Cy5.5 anti-human CD3	BD Biosciences	Cat# 560835; RRID:AB_2033956
BV711 anti-human CD31	BD Biosciences	Cat# 740777; RRID:AB_2740440
BV510 anti-human CD73	BD Biosciences	Cat# 563198; RRID:AB_2738062

(*Continued on next page*)

CellPress
OPEN ACCESS

Continued

REAGENT or RESOURCE	SOURCE	IDENTIFIER
PE anti-human IL-3	BD Biosciences	Cat# 554676; RRID:AB_395504
Rat IgG-PE	Biolegend	Cat# 400408; RRID:AB_326514
Alexa Fluor 488 anti-human CD105	Biolegend	Cat# 323209; RRID:AB_755961
PE-Dazzle anti-human gp38	Biolegend	Cat# 337027; RRID:AB_2750287
Rat anti-mouse Ly6G	Biolegend	Cat# 127632; RRID:AB_11150581
Rat anti-mouse CCL5	R&D systems	Cat# MAB478-100; RRID:AB_2290968
Rat anti-mouse CCL20	R&D systems	Cat# MAB7601-100; RRID:AB_2071906
Rat anti-mouse CXCL1	R&D systems	Cat# MAB453-100; RRID:AB_2087696
Goat anti-mouse CXCL2	R&D systems	Cat# AF-452-NA; RRID:AB_2086326
Rat IgG2a	R&D systems	Cat# MAB006; RRID:AB_357349
Rat IgG2a	Biolegend	Cat# 400544; RRID:AB_11147167
Goat IgG	R&D systems	Cat# AB-108-C; RRID:AB_354267
Rat IgG1	R&D systems	Cat# MAB005; RRID:AB_357348
Goat anti-human CD123	Abcam	Cat# ab205365; RRID:AB_2747492
Rabbit anti-human EpCAM	Abcam	Cat# ab71916; RRID:AB_1603782
Bacterial and virus strains		
Salmonella Typhimurium	Prof. J. Mattner (Erlangen, Germany)	Strain SL1344
Chemicals, peptides, and recombinant proteins		
Dextran sulfate sodium	MP Biomedicals	02160110
4-Ethoxymethylen-2-phenyl-2-oxazolin-5-on	Sigma-Aldrich	862207
Recombinant IL-3	R&D systems	403-ML-025/CF
Haematoxylin Gill-III	Merck	1.05174
Eosin Y solution	Merck	318906
CM-H2DCFDA	ThermoFischer	C6827
Phorbol 12-myristate 13-acetate (PMA)	Sigma-Aldrich	P1585
Dimethyl sulfoxide (DMSO)	ThermoFischer	D12345
STATIC	MERCK	S7947-25MG
N'-((4-Oxo-4H-chromen-3-yl) methylene) nicotinohydrazide, 98%	BLD Pharm.	BD767885 98%
Critical commercial assays		
Neutrophil Isolation Kit	Miltenyi Biotec	130-097-658
Elisa kits for murine TNFα	Biolegend	430904
QIAsymphony RNA kit	Qiagen	931636
SMART-Seq® v4 Ultra® Low Input RNA Kit for Sequencing	Takara bio	634891
Qubit dsDNA HS Assay-Kit	ThermoFischer	Q32854
Nextera XT Library Preparation kit	Illumina	FC-131-1024
RNeasy mini kit	Qiagen	74106
Deposited data		
RNA-seq data (spleen vs BM neutrophils)	This publication	SRA: SRP375072
Experimental models: Organisms/strains		
Mouse: BALB/c	Janvier-labs	N/A
Mouse: BALB/c *Il-3*^{−/−}	RIKEN BRC Laboratories	RBRC02298
Mouse: C57BL/6	Janvier-labs	N/A
Mouse: C57BL/6 *Il-3*^{−/−}	This paper	N/A
Mouse: *Cd131*^{−/−}	The Jackson laboratory	RRID:IMSR_JAX:005940
Mouse: SCID	Janvier-labs	N/A

(Continued on next page)

REAGENT or RESOURCE	SOURCE	IDENTIFIER
Continued		
Oligonucleotides		
Murine *Ccl20* primer	ThermoFischer	Mm01268754_m1
Murine *Il-3* primer	ThermoFischer	Mm00439632_g1
Human *GAPDH* primer	ThermoFischer	Hs00266705_g1
Human *CD123* primer	ThermoFischer	Hs_IL3_1_SG QuantiTect Primer Assay; Cat# 249900
Human *CCL5* primer	ThermoFischer	Hs00174575_m1
Human *IL-3* primer	Qiagen	Hs00608141_m1
Software and algorithms		
FlowJo 10.8.1	FlowJo LLC	RRID:SCR_008520
CFX Manager	Bio-Rad	RRID:SCR_017251
GraphPad Prism	GraphPad Software	RRID:SCR_002798
NextGenMap	N/A	RRID:SCR_005488
featureCounts	N/A	RRID:SCR_012919
DESeq2	N/A	RRID:SCR_015687

RESOURCE AVAILABILITY

Lead contact
Further information and requests for resources and reagents should be directed to and will be fulfilled by the lead contact, Alan Bénard (alan.benard@uk-erlangen.de).

Materials availability
This study did not generate new unique reagents.

Data and code availability
- RNA-seq data have been deposited at NCBI Sequence Read Archive and are publicly available as of the date of publication. Accession number is listed in the key resources table.
- This paper does not report original code.
- Any additional information required to reanalyze the data reported in this work paper is available from the lead contact upon request.

EXPERIMENTAL MODEL AND STUDY PARTICIPANT DETAILS

Animals
All animal protocols were approved by the animal review committee from the university hospital Erlangen and the local governmental animal committee (Protocol number: 55.2-2532-2-837 and 55.2-2532-2-1221). BALB/c (WT), C57BL/6J (WT) (Janvier, Le Genest-Saint-Isle, France), *Cd131-/-* (C57BL/6 background, bred in-house), *Il-3-/-* (BALB/c background; obtained from RIKEN BRC Laboratories, Japan), C57BL/6J *Il-3-/-* (bred in-house) and Severe combined immunodeficient mice (SCID; Janvier) male and female mice were used in this study. Mice were 8-12 weeks old when used for experiments. All mice were bred in the same facility, and age and sex of WT mice matched with genetically modified mice. Purchased mice were acclimated to their new environment for at least one week before starting experiments. Mice were breed in animal facility where i) air exchange rate of up to 30 times per hour is possible in the animal rooms; ii) the animals are subject to a 12 h light/dark rhythm; iii) air humidity is between 45 and 65%; iv) the temperature is 20 and 24°C; v) the animals receive autoclaved and autoclavable water; and vi) food and water are ad libitum. Mice with severe pain were removed from the experiments and sacrificed to prevent additional suffering as well as mice death, accordingly to the cumulative termination criteria of our ethical protocol.

Disease severity index
Animals were evaluated daily for stool consistency, bleeding and weight loss. Scoring of disease severity were designed as follow: *stool consistency*: 0: normal, 1: slightly loose, 2: watery stool, 3: diarrhea; *bleeding*: 0: no bleeding, 1: hemoccult positive, 2: few blood-tinged stools, 3: rectal bleeding; *weight loss*: 0: none, 1: 1-5%, 2: 5-10%, 3: 1015%, 4: >15%.

Mouse treatment
DSS-induced colitis
DSS (MP Biomedicals) was dissolved in drinking water at 3% w/v (C57BL/6J) or 5% w/v (BALB/c) and the animals were free to drink the DSS solution for a maximum of 7 days. No differences were reported for the volume consumed between the different genetic backgrounds. At the indicated time, mice were sacrificed and organs were harvested for further analyses.

Oxazolone-induced colitis
Colitis was induced by oxazolone as previously described.[47] Mice were sensitized by epicutaneous application of 1% oxazolone (4-ethoxymethylene-2-phenyl-2-oxazolin-5-one; Sigma-Aldrich) dissolved in a mixture of acetone and oil (4:1) on day 0, followed by intra-rectal administration of 1% oxazolone dissolved in 50% ethanol on day 8.

Salmonella Typhimurium infection
Salmonella infection was performed as previously described.[48] Briefly, BALB/c and *Il-3*-deficient mice received 20 mg streptomycin orally. 6 hours later, mice were infected by oral gavage with 10^5 or 10^6 CFUs of wild-type *Salmonella* (SL1344) in 100 μL PBS (pH 7.3). 4 days post-infection, feces and organs were harvested and bacterial burden was assessed by limiting dilution assays.

I.v. antibody injection
Mice were anesthetized with isoflurane and 200μg of rat anti-Ly6G (Biolegend) or 12.5μg of rat anti-CCL5 (R&D systems, Minneapolis, MN, USA), rat anti-CCL20 (R&D systems) or a cocktail of rat anti-CXCL1 and goat anti-CXCL2 (R&D systems) were injected intravenously (100μl) just before DSS treatment. Corresponding isotype were used as controls. *IL-3 injection:* PBS or 300ng of recombinant IL-3 was i.p. injected (100μl) in *Il-3$^{-/-}$* mice 12h before DSS treatment, at the onset and 12h after.

Adoptive transfer
Neutrophils from splenic or BM were purified by negative selection using the Neutrophil Isolation Kit (Miltenyi Biotec, Bergisch Gladbach, Germany) and were injected intravenously (2×10^6 cells in 100μl) 3h after the onset of DSS-induced colitis.

Splenectomy
Under isoflurane anesthesia, the left part of the abdominal cavity of the mice was opened and the spleen vessels were ligated using a 7.0 thread (Ethilon, Bridgewater, NJ and Cincinnati, OH, USA). The spleen was then carefully removed. For control experiments (sham), the abdomen was opened without removing the spleen. Then the abdomen was closed with a continuous suture (5.0 thread, Ethilon). Then, mice recovered for at least 1 week before inducing colitis.

STAT3/5 inhibition
STAT3 (STATTIC; MERCK) and STAT5 (N'-[(E)-(4-oxo-4H-chromen-3-yl)methylidene]nicotinohydrazide; BLD pharm, Shanghai, China) inhibitors were intraperitoneally injected (10 mg/kg) just before DSS treatment.

Human
The study was performed at the University of Erlangen in Germany and agreed with the local ethics review board of the University Hospital of Erlangen (UKER 339_15 Bc, UKER 10_16 B, UKER 180_19 B). Patients' confidentiality was maintained and informed consent was obtained from all subjects. A summary of sex/gender and age of study participants can be found in Table S1. Patients were chosen without considering their sex, gender or diversity. As well, patients were recruited without considering their ancestry, race or ethnicity.

METHOD DETAILS

Murine leukocyte isolation
After colon harvest, single cell suspensions were obtained as follow: perfused colon were cut in small pieces and subjected to enzymatic digestion with 450 U/ml collagenase I (Sigma Aldrich), 125 U/ml collagenase IX (Sigma Aldrich), 60 U/ml hyaluronidase (Sigma Aldrich), 60 U/ml Dnase (Sigma Aldrich), and 20 mM Hepes (Thermo Fisher Scientific, Waltham, MA, USA) for 1 h at 37°C while shaking. Spleens were homogenized through a 40 μm nylon mesh and bone marrow (BM) cells were flushed out of the femurs and tibias. Neutrophils from spleen and BM were purified by negative selection using Neutrophil Isolation Kit (Miltenyi Biotec, Bergisch Gladbach, Germany), according to the manufacturer's instructions with two subsequent passages on the columns (Miltenyi Biotec). Purity was >98% for neutrophils from BM and >90% for splenic neutrophils. Purified neutrophils were then cultured (106 cells/ml) in RPMI-1640 GlutaMax supplemented with 10% FCS, 25mM of Hepes, 1 mM sodium pyruvate, 100U/ml of Penicillin-Streptomycin and stimulated by 0.5μg/ml of LPS (Sigma-Aldrich, Saint-Louis, MO, USA) during 4h in presence or in absence of Golgi Plug (BD Biosciences, Franklin Lakes, NJ, USA).

Human blood and tissue samples and leukocyte isolation
Blood
After blood collection, plasma of healthy donors and patients with UC were immediately obtained by centrifugation, transferred into cryotubes, and stored at −80°C until further processing.

Colon
Colons from patients with ulcerative colitis (n=16) were obtained by resecting inflamed colon sections (Table S1). Control colons were healthy tissue obtained from the colon resection of patients with colorectal cancer (n=13) (Table S1). Subsequently, tissue samples

were taken from the surgically removed material and transported into the laboratory under standardized conditions (at 4°C, in Ringer's solution). Single cell suspensions of colon were obtained as follow: colons were cut in small pieces and subjected to enzymatic digestion with 450 U/ml collagenase I, 125 U/ml collagenase IX, 60 U/ml hyaluronidase, 60 U/ml Dnase, and 20 mM Hepes for 1 h at 37°C while shaking. The inflammation levels low (+) and high (++) were assessed through the expression of *TNF* and the percentage of neutrophils in the colon. Not every sample could be used for all analyses.

Ex vivo colon stimulation by IL-3
Ex vivo colon stimulation were performed as previously described.[49] After colon harvest, the contents of the lumen were washed with ice-cold PBS, cut longitudinally into 2 parts and washed again in ice-cold PBS in a Petri dish. Then, each part of the colon was cut into sections of 1 cm long and transferred into separate cell strainers (100 μm) placed on wells of a 6-well culture plate with 5 sections per well. Sections were recovered with RPMI-1640 GlutaMax supplemented with 5% FCS, 100U/ml of Penicillin-Streptomycin and 20 μg/ml of Gentamicin and incubated at 37°C in the presence of 5% CO2. After 2h, colon sections were washed 3 times with medium without any antibiotics. Then, colon sections were transferred into wells of a 12-well plate containing 1 mL of medium without any antibiotics and 40 ng/ml of recombinant IL-3 (R&D systems). After 24h, colon sections were harvested and processed for quantitative RT-PCR analysis.

Chemotaxis assays
Neutrophil chemotaxis was performed using 24-well Transwell plates (Corning) with a 3 μm pore size polycarbonate filter. Splenic neutrophils (10^5 cells) were added to the upper chamber of the Transwell unit, and 1% FBS RPMI-1640 medium, with or without chemoattractants, was added to the lower chamber. After incubating the chambers for 1 hour at 37°C, the transmigrated cells were collected from the lower chamber and counted on a flow cytometer.

Mixed bone-marrow chimera
Naive WT and *Il-3*$^{-/-}$ mice were lethally irradiated (7.5 Gy) using a γ-irradiator BioBeam and reconstituted with a total 5 x 10^6 donor derived bone-marrow cells from WT or *Il-3*$^{-/-}$ mice. Chimeric mice were treated with broad spectra antibiotics (Baytril, Bayer, Leverkusen, Germany) in the drinking water until full reconstitution of the hematopoietic system (6-8 weeks).

Histology
Tissue sections with 4 μm were cut from formalin-fixed paraffin embedded (FFPE) murine colons and stained by haematoxylin/eosin. In brief, the sections were dewaxed using two times xylol for 10 min followed by rehydration in a decreasing ethanol row. After a wash in A.d. the sections were stained by haematoxylin Gill-III (1:3 diluted, Merck) for 3.5 min, followed by 10 min warm tap water. Subsequently, staining for 1 min in eosin Y solution (Sigma) and two times washing in A.d. for 5 min followed. Slides were subjected to an increasing ethanol row and finally mounted using VectaMount Permanent Mounting medium (Vector Laboratories).

Immunohistochemistry
For CD123 and EpCAM permanent immunohistochemistry, formalin-fixed, paraffin-embedded tissue were deparaffinized by xylene two times for 15 min. The tissue was rehydrated using decreasing concentrations of ethanol (100%, 96%, 85%, 70%) for 2 min each. Antigen retrieval was performed using Target Retrieval Solution (DakoCytomation) at pH 9.0 at 95°C for 20 min followed by cooling for 20 min at RT. As a washing buffer between the incubation steps 1xTBS pH 7.6 was used. The slides were blocked by hydrogen peroxide (7.5%, Sigma-Aldrich), followed by avidin-biotin-block (Vector Laboratories), and subsequent 2.5% horse normal serum block (HNS, Vector Laboratories) in 1xTBS for 10 min. The primary antibody diluted in 2.5% HNS (goat anti-human CD123 cat. no. ab205365, Abcam, 1:300; rabbit anti-human EpCAM cat no. ab71916, Abcam,1:300) and isotype control antibody in corresponding concentration were detected using the ImmPRESS HRP Reagent Kit anti-Goat (Vector Laboratories) and NovaRed substrate (Vector Laboratories) as a substrate. The slides were counterstained with Gill-III hematoxylin (1:3 diluted, Merck), dehydrated and mounted with VectaMount permanent mounting medium (Vector Laboratories). The sections were analyzed using a DM6000 B microscope (Leica).

RNA-seq
RNA extraction
Neutrophils from spleen and BM were cell sorted using a MoFlo Astrios EQ cell sorter (Beckman Coulter, Brea, CA, USA) directly into RNA lysis buffer. RNA isolation was performed using the QIAsymphony (Qiagen, Hilden, Germany) with the QIAsymphony RNA kit according to the manufacturer's protocol. Samples were thawed, filled up to a volume of 400 μL with Roti®-Stock PBS (Carl Roth, Karlsruhe, Germany) and loaded for QIAsymphony extraction. Extracted RNA was eluted in 100 μL buffer (Qiagen, Hilden, Germany). 180 μL Agencourt RNAclean XP beads (Beckman Coulter, Krefeld, Germany) were used for further purification. Finally, RNA was eluted in 20 μL nuclease-free water. Quantity and quality of isolated RNA were determined with the Qubit High Sensitivity RNA kit (Thermo Fisher Scientific, Langenselbold, Germany) and the Ultra Sensitivity RNA Kit using Femto Pulse (Agilent Technologies, Waldbronn, Germany).

Preparation of NGS libraries and sequencing

Synthesis of cDNA was accomplished by SMART-Seq v4 Ultra Low Input RNA kit for sequencing (Takara Bio, Gothenburg, Sweden). One nanogram of total RNA was used for first-strand synthesis. Full-length cDNA was generated via template switching (SMART) and PCR was performed according to the manufacturer's protocol. Quantification of cDNA was done using the Qubit dsDNA HS Assay kit (Thermo Fisher Scientific, Langenselbold, Germany). Libraries for NGS were prepared from one nanogram cDNA using the Nextera XT Library Preparation kit (Illumina, San Diego, USA). After tagmentation, barcodes were ligated and PCR was performed. With the exception that final elution after bead purification was carried out with 34 μL of resuspension buffer, sample preparation was performed according to the manufacturer's protocol (Illumina, San Diego, USA). Libraries were quantified by Qubit dsDNA HS Assay kit (Thermo Fisher Scientific, Langenselbold, Germany) and quality was assessed using the High Sensitivity NGS kit on a Fragment Analyzer (Agilent, Waldbronn, Germany). Sequencing of libraries was performed on NextSeq2000 (Illumina, San Diego, USA), resulting in 40 million 100-bp single-end reads per sample.

Differential gene expression analysis

Raw sequencing reads were processed with BBTools (bbduk.sh) to remove sequencing artifacts and poor-quality reads.[50] Reads were mapped against the murine reference genome assembly GRCm38 using NextGenMap (v. 0.5.5) with default settings.[51] Gene quantification in raw read counts was carried out exclusively with uniquely mapped reads using featureCounts (v 2.0.1) with a gene annotation from Ensembl (Mus_musculus.GRCm38.79).[52] Identification of differentially expressed genes (DEGs) was done with the R package DEBrowser (v. 1.2.0) using the implemented DESeq2 method and default settings.[53,54] Genes with less than one read in any of the replicates were removed before analysis with DESeq2. Genes were considered as differentially expressed between two conditions with an adjusted p-value (FDR, false discovery rate) ≤ 0.01 and a fold change ≤ -2 or ≥ 2. Volcano plots and heatmaps were also created using DEBrowser. For the heatmap, a pseudo-count of 0.1 was added to the values to apply log2 scaling, and values were column centered with a Z-score. Differential genes and samples were hierarchically clustered and divided into two groups based on the correlation between samples with complete-linkage clustering.

Neutrophil function assays

Reactive oxygen species assay

Isolated murine bone marrow and spleen cells were incubated for 20min at 37°C and 5% CO2 with 2μM of the general oxidative stress indicator CM-H2DCFDA (Thermo Fisher) in R0 medium, consisting of RPMI-1640 medium (Gibco Thermo Fisher Scientific, 11835-063) supplemented with 1% of penicillin-streptomycin (Gibco, 15140-122) and L-glutamine (Gibco,26030-024). After a washing step to remove surplus CM-H2DCFDA (5min, 659xg), the cell count was adjusted to 500,000 cells/ml in R0 medium containing 10% fetal calf serum (Gibco, 10270-106, heat inactivated, 30min 56°C). Cell stimulation was achieved by addition of 100ng/ml phorbol 12-myristate 13-acetate (PMA) (Sigma-Aldrich), or dimethyl sulfoxide (Thermo Fisher) in the same dilution as control. The cell suspension was incubated with the stimuli for 30min at 37°C and 5% CO2 in a humidified atmosphere. The cells were then stained and the FL1 fluorescence of CD11b⁺Ly6G⁺F4/80⁻ cells was analyzed by flow cytometry.

Neutrophil elastase activity

Neutrophil elastase (NE) activity in supernatants of LPS-stimulated neutrophils from spleen and bone-marrow was determined by the conversion of the fluorogenic NE-substrate (MeOSuc-AAPV-AMC, ENZO, BML-P224-0005; Ex: 380nm, Em: 460nm) for 3 hours at 37°C, using the plate reader Infinite F200 Pro fluorometer (TECAN, Männedorf, Swiss). Fluorescence was recorded every 10 min. The levels of elastase activity were assessed as follow: after subtracting the background (sample without substrate), each time points were compared to the reference point (t0).

Quantitative RT-PCR

Real-time PCR was performed as previously described.[55] Briefly, RNA was extracted from cells by RNeasy mini kit (Qiagen, Venlo, Netherlands). Complementary DNA was reverse transcribed from 1 μg total RNA with Moloney murine leukemia virus reverse transcriptase (Thermo Fisher Scientific) using random hexamer oligonucleotides for priming (Thermo Fisher Scientific). The amplification was performed with a Biorad CFX-Connect Real-time-System (Thermo Fisher Scientific) using the PCR SYBR Green sequence detection system (Eurogentec, Seraing, Belgium), the QuantiTect Primer Assay (Qiagen) or Taqman (Thermo Fisher Scientific). Data were analyzed using the software supplied with the Sequence Detector (Life Technologies). The mRNA encoding for murine *Tnfα* and *Ccl5* were normalized to the hypoxanthine-guanine phosphoribosyltransferase (Hprt) mRNA. Gene expression was quantified using the ΔΔCt method (except for Figures 1A–1D and 5B). The expression level was arbitrarily set to 1 for one sample from the control group and the values for the other samples were calculated relatively to this reference (except for Figures 1A–1D and 5B). Primers for murine *Ccl20* and *Il-3* as well as primers for human *GAPDH*, *CD123* and *CCL5* were designed by Thermo Fisher Scientific. Primers for human *IL-3* were designed by Qiagen. The sequence of the other primers is in Table S2.

Cytokine detection

Secreted murine TNFα (Biolegend, San Diego, CA, USA) was measured by ELISA according to the manufacturer's instructions.

Flow cytometry

The following antibodies were used for flow cytometric analyses: *Mouse*: anti-CD19-PE (1D3, BD Biosciences), anti-CD11b-PE CF594 (M1-70, BD Biosciences), anti-CD11c-PE (HL3, BD Biosciences), anti-CD49b-PE (DX5, BD Biosciences), anti-CD90.2-PE (53-2.1, BD Biosciences), anti-B220-PE (RA3-6B2, BD Biosciences), anti-Ter119-PE (Ter-119, BD Biosciences), anti-CD127-PE (SB/199, Biolegend), anti-Gr1-PE (RB6-8C5, Biolegend), anti-SCA-1-BV711 (D7, BD Biosciences), anti-c-Kit-BV605 (ACK2, Biolegend), anti-CD34-FITC (RAM34, BD Biosciences), anti-CD16/32-BUV395 (2.4G2, BD Biosciences), anti-CD115-PerCP Cy5.5 (AFS98, Biolegend), anti-CD326-BV650 (G8.8, BD Biosciences), anti-Ly6C-FITC (AL-21, BD Biosciences), anti-CD11b-BUV737 (M1/70, BD Biosciences), anti-MHCII-BV711 (M5/114.15.2, BD Biosciences), anti-F4/80-BV510 (T45-2342, BD Biosciences), anti-Ly6G-BUV395 (1A8, BD Biosciences), anti-CD19-BV421 (1D3, BD Biosciences), anti-CD3-PerCP Cy5.5 (17A2, BD Biosciences), anti-CD138-PerCP Cy5.5 (281-2, Biolegend), anti-CD45.2-BV786 (104, BD Biosciences), anti-CD43-FITC (S7, BD Biosciences), anti-IgM-BV650 (R6-60:2, BD Biosciences), anti-CD5-BV510 (53-7.3, BD Biosciences), anti-MHCII-BV711 (M5/114.15.2, BD Biosciences), anti-CD93-BUV395 (AA4.1, BD Biosciences), anti-CD3-BV650 (145-2C11, BD Biosciences), anti-CD3-PE-Dazzle (17A2, Biolegend), anti-TCRβ-FITC (H57-597, BD Biosciences), anti-CD8-BV711 (53-6.7, BD Biosciences), anti-CD4-BUV395 (GK1.1, BD Biosciences), anti-TCRγδ-BV421 (GL3, BD Biosciences), anti-CD31-Pacific Blue (390, Biolegend), anti-CD73-PerCP Cy5.5 (Ty/11.8, Biolegend), anti-CCR1-PE (S15040E, Biolegend), anti-CCR3-FITC (J073E5, Biolegend), anti-CCR5-PerCP-Cy5.5 (HM-CCR5, Biolegend), anti-CCR6-BV786 (29-2L 17, Biolegend), anti-CXCR4-PE-Dazzle (L276F12, Biolegend), anti-CD62L-Pacific Blue (MEL-14, BD Biosciences), anti-PD-L1-PerCP Cy5.5 (10F.9G2, BD Biosciences), anti-CD64-BV711 (X54-5/7.1, Biolegend), anti-gp38-FITC (8.1.1, Biolegend), anti-CD54-PerCP-Cy5.5 (YN1/1.7.4, Biolegend), anti-CD106-BUV395 (429, BD Biosciences), anti-CD105-Pacific Blue (MJ7/18, Biolegend), anti-CD44- PerCP-Cy5.5 (IM7, Biolegend), anti-CD25-FITC (3C7, Biolegend), anti-CD223-FITC (C9B7W, Biolegend), anti-PD-1- PerCP-Cy5.5 (29F.1A12, Biolegend), anti-CCR7- PE/Dazzle 594 (4B12, Biolegend), anti CD123-PE (5B11, Biolegend), IgG2a-PE (RTK2758, Biolegend), anti-CCL5-PE (2E9/CCL5, Biolegend), IgG2b-PE (MPC-11, Biolegend), anti-IL-3-PE (MP2-8F8, BD Biosciences), IgG1-PE (R3-34, BD Biosciences), anti-IL-1β-e450 (NJTEN3, Thermofischer), IgG1-ebio (eBRG1, Thermofischer), anti-TNFα- PerCP Cy5.5 (MP6-XT22, BD Biosciences), IgG-PerCP Cy5.5 (R3-34, BD Biosciences), anti-IL-10-BV650 (JES5-16E3, BD Biosciences), IgG2-BV650 (B81-3, BD Biosciences), anti-IFNγ-BUV737 (XMG1.2, BD Biosciences), IgG2a- BUV737 (R35-95, BD Biosciences), anti-IL-17A-BV785 (TC11-18H10.1, Biolegend), IgG1-BV785 (RTK2071, Biolegend), anti-CXCL1-Alexa Fluor 488 (1174A, R&D Systems), IgG- Alexa Fluor 488 (60024B, R&D Systems), anti-CCL2-Alexa Fluor 405 (123616R, R&D Systems), IgG2b- Alexa Fluor 405 (141945, R&D Systems), anti-CCL3-Alexa Fluor 488 (39624, R&D Systems), IgG2a-Alexa Fluor 488 (54447, R&D Systems) or anti-Ki-67-PE dazzle (16A8, Biolegend). *Human*: anti-CD14-BUV737 (M5E2, BD Biosciences), anti-CD15-BV421 (W6D3, Biolegend), anti-HLADR-PerCP-Cy5.5 (G46-6, BD Biosciences), anti-CD16-FITC (3G8, Biolegend), anti-CD64-PE (10.1, Biolegend), anti-CD11c-BV711 (B-ly6, BD Biosciences), anti-CD19-BUV395 (SJ25C1, BD Biosciences), anti-CD45-BV786 (HI30, BD Biosciences), anti-CD3-BV510 (UCHT1, BD Biosciences), anti-CD326-B650 (9C4, Biolegend), anti-CD123-PE-CF594 (7G3, BD Biosciences), IgG2a-PE-CF594 (G155-178, BD Biosciences), anti-CD3-PerCP-Cy5.5 (UCHT1, BD Biosciences), anti-CD31-BV711 (WM59, BD Biosciences), anti-CD73-BV510 (AD2, BD Biosciences), anti-IL-3-PE (BVD3-1F9, BD Biosciences), IgG-PE (RTK2071, Biolegend), anti-CD105-Alexa Fluor 488 (43A3, Biolegend), anti-gp38-PE Dazzle (NC-08, Biolegend). Intracellular staining was performed using BD Cytofix/Cytoperm Plus Kit (BD Biosciences). Data were acquired on a CytoFLEX Flow Cytometer (Beckman Coulter) or on a Celesta (BD Biosciences) flow cytometer and analyzed with FlowJo (v 10.8.1) (FlowJo LLC, Ashland, OR, USA).

QUANTIFICATION AND STATISTICAL ANALYSIS

Results were expressed as mean ± S.E.M. All statistical analyses were performed using Prism (GraphPad, RRID:SCR_002798). Statistical details of experiments and sample numbers can be found in the figure legends. Significance is stated as follows: *p < 0.05, **p < 0.01, ***p < 0.001. Significant outliers were determined using GraphPad Prism 7.0 software and excluded from the analysis.